IL-4Rα without inducing signal transduction, and has no detectable activity upon the proliferation or differentiation of murine cells. An appropriate amount of IL-4DM completely inhibits responses by wild-type IL-4.[19] Like its human analogue, the IL-4DM mutant is also an antagonist of IL-13 (B. Schnarr et al., unpublished data[37]). Recent experiments with monocytes from mice lacking a functional γc gene showed that IL-4DM is a complete inhibitor of IL-4 in the absence of γc as well.[20] In this study we have examined the effects of IL-4DM in vivo, using an AD model induced by the repeated exhibition of oxazolone (OX). The repeated application of a hapten such as OX on mice causes an initial delayed-type hypersensitivity that changes to an immediate-type response in the late phase with elevated IgE production and deviation of Th-cell responses. The skin lesions that appear in the late phase are compatible with the clinical findings as well as the cytokine profile observed in AD.[21–23] The inhibitory effect of IL-4DM on IL-4 and IL-13 on the immune response was comparable with that of knockout mice lacking either IL-4[24] or IL-4Rα. Treatment with IL-4DM prevented contact hypersensitivity responses with the increased production of interferon (IFN)-γ.

Materials and methods

Animals

BALB/c male mice aged 5 weeks were purchased from Japan SLC Co. (Shizuoka, Japan) and were used at the age of 6 weeks. Age-matched wild-type BALB/c mice were used as controls. All animals were cared for according to the ethical guidelines approved by the Institutional Animal Care and Use Committee of Mie University.

Reagents

The cDNA coding region of mouse IL-4 was amplified by a polymerase chain reaction (PCR) based on the cDNA sequence of mouse IL-4. The mouse IL-4 fragment was inserted into BamHI and EcoRI-filled in pcDNA3.1+ (Invitrogen, San Diego, CA, U.S.A.) under the TPA leader sequence, and then digested by BamHI and SacI. A Quickchange™ Site-directed Mutagenesis kit (Stratagene, La Jolla, CA, U.S.A.) was used for the mutagenesis of mouse IL-4. The oligonucleotide primers used to prepare a mouse IL-4 double mutant (IL-4DM, Q116D/Y119D) were CTAAAGAGCATCATGGATATGGATGACTCGTAGTCTAGAG and CTCTAGACTACGAGTCATCCATATCCATGATGCTCTTTAG. The IL-4 mutant fragments were ligated into pcDNA3.1+.[25] Mouse IL-4, IL-4DM plasmid DNAs were purified using the Plasmid Mega kit (Qiagen, Chatsworth, CA, U.S.A.) and diluted with sterilized physiological saline. OX was purchased from Sigma (St Louis, MO, U.S.A.) and was dissolved in acetone/olive oil (4 : 1).

Administration of DNA

Mice were treated by intraperitoneal injection of 100 μg of IL-4DM DNA on days 0, 7, 14, 21 and 28. A control plasmid (pcDNA3.1+) vector and IL-4 DNA were also injected on the same day (Fig. 1).

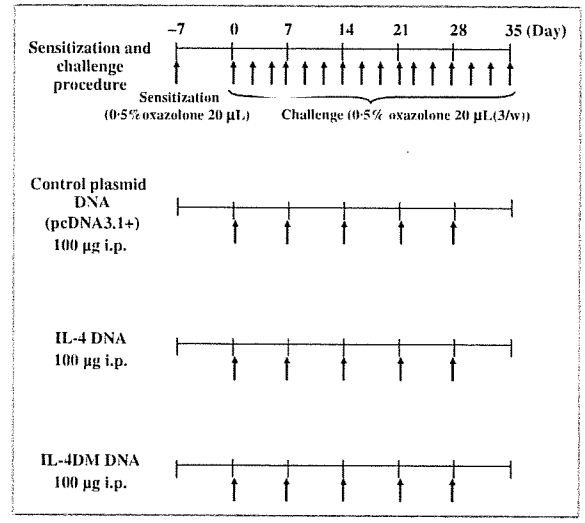

Fig 1. Schedule for induction of chronic contact hypersensitivity and administration of compounds. Mice received intraperitoneal (i.p.) injection of 100 μg of each plasmid DNA on days 0, 7, 14, 21 and 28.

Sensitization and challenge procedures

As shown in Figure 1, mice were initially sensitized by pasting 20 μL of 0·5% OX solution to their left ear 7 days before the first challenge (day 7) and then 20 μL of 0·5% OX solution was repeatedly applied on the left ear three times per week from day 0 as reported previously.[23] Ear swelling was measured with thickness gauge calipers before and 30 min after OX challenge to the pinna of the ear on day 35. The ear swelling response was expressed as the difference between the values taken before and 30 min after application.

Histological analysis

Ear skin specimens obtained 6 h after the final challenge on day 35 were fixed in 10% buffered neutral formaldehyde and embedded in paraffin wax. Histological sections were of 6 μm thickness and they were stained with haematoxylin and eosin. The sections were also stained with 0·5% toluidine blue for the identification of mast cells. The cell counts were performed in six consecutive microscopic fields at × 400 magnification.

Measurement of plasma IgE and plasma histamine

Blood was collected under ether anaesthesia 6 h after the last challenge. Plasma IgE levels were determined by a sandwich enzyme-linked immunosorbent assay (ELISA). In brief, 96-well immunoplates (Corning Inc., Corning, NY, U.S.A.) were coated with 100 μL of an antimouse IgE capture antibody (2 μg mL^{-1}) (BD PharMingen, San Diego, CA, U.S.A.) overnight at 4 °C. Plasma samples of 100 μL were diluted 60-fold with PBS

containing 10% fetal calf serum (FCS) were placed in the wells. After incubation for 1 h at room temperature, 100 μL of biotin-conjugated antimouse IgE antibody (2 μg mL^{-1} in blocking buffer) (BD PharMingen) was added to each well. The plates were incubated at room temperature for 1 h, followed by six washes, incubated with 100 μL of horseradish peroxidase avidin D (FUNAKOSHI, Tokyo, Japan) 1 : 1000 in blocking buffer, and then incubated for 30 min at room temperature. A substrate solution of 100 μL containing 1·5 mg ABTS (Sigma-Aldrich, St Louis, MO, U.S.A.) in 5 mL of a 0·1 mol L^{-1} citric acid solution was added, and kept for 30 min at room temperature in a dark place. Thereafter the reaction was terminated by adding 50 μL of 2 mol L^{-1} H_2SO_4, and the optical density of each well at 405 nm was determined by using a microplate reader. A standard curve was prepared using mouse anti-TNP IgE standard (BD PharMingen). Plasma histamine levels were analysed using the commercial sandwich ELISA kit from Immunoteck (Marseille, France) according to the manufacturer's protocol.

Purification of mRNA from mouse ears

At 6 h after the final challenge, the skin of the left ear was sampled. The specimen was homogenized and the total RNA was extracted using Isogen (Nippon Gene, Tokyo, Japan) according to the manufacturer's instruction; 1 mL of homogenate was vigorously mixed with 200 μL of chloroform, and centrifuged at 12 000 *g* for 15 min at 4 °C. The aqueous phase was separated and mixed with 0·5 mL of 2-propanol (Nacalai Tesque, Kyoto, Japan) to precipitate RNA. After centrifugation, the precipitate was washed with 1 mL of 75% ethanol (Nacalai Tesque) and dried. RNA was suspended in 50 μL of RNase-free water, and the concentration was measured based on the absorbance at 260 nm, and the quality was confirmed by electrophoresis. cDNA was prepared from 10 μg of mRNA using archive kit (ABI, Foster City, CA, U.S.A.) according to the manufacturer's protocol.

Cytokine mRNA expression in skin

The transcriptional activity in the lesional skin samples was measured with a PCR. The amplification of cDNA was performed in 50 μL of a master mixture containing 0·5 μg of cDNA, 200 nmol deoxynucleotide triphosphate, 5 μL of PCR buffer, 2 U of Taq polymerase (ABI) and 2 μmol of each specific primer for the DNA of interest. The following primers were used for PCR reactions (5′–3′), mouse IFN-γ: TCAAGTGGCATAGATGTGGAAGAA and TGGCTCTGCAGGATTTTCATG; mouse IL-2: CCTGAGCAGGATGGAGAATAACA and TCCAGAACATGCCGCAGAG; mouse IL-4: CACTGACGGCACAGAGCTATTGATG and TCATGGTGCAGCTTTCGATGAATC; mouse IL-10: CTCTTACTGACTGGCATGAGGATCAGCAGG and TCTTCACCTGCTCCACTGCCTTGCTCTTAT; mouse IL-12: TCCTGCACTGCTGAAGACATC and TCTCGCCATTATAGATTCAGAGAC; mouse IL-13: AGACCAGACTCCCCTGTGCA and TGGGTCCTGTAGATGGCATTG; mouse β-actin: TGGAATCCTGTGGCATCCATGAAAC and TAAAACGCAGCTCAGTAACAGTCCG.[26] PCR was performed under the following conditions: 95 °C for 5 min, followed by 35 or 40 cycles of 95 °C for 30 s, 56 °C (IFN-γ, IL-12) or 60 °C (IL-2, IL-4, IL-10, IL-13, β-actin) for 30 s, and 72 °C for 1 min were carried out. After the final cycle, the temperature was maintained at 72 °C for 7 min. PCR amplified fragments were electrophoresed through 1·5% agarose gels in tris-acetate EDTA buffer containing ethidium bromide, and the gels were scanned under ultraviolet light. The mRNA of β-actin was used as an internal control. The signal intensity of each reverse transcriptase (RT)-PCR product was estimated using an ATTO Lane & Spot Analyzer (ATTO, Shizuoka, Japan).

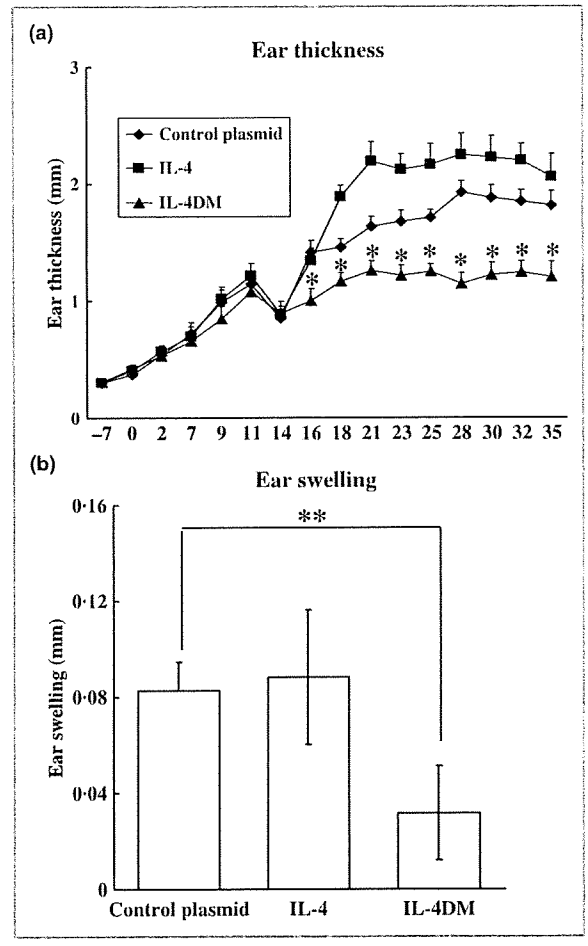

Fig 2. The effects of interleukin (IL)-4DM, IL-4, and control plasmid (pcDNA3.1) on ear swelling induced by repeated application of oxazolone (OX). (a) Ear thickness was measured before each OX challenge. Each point represents the mean ± SD of seven or eight mice. *$P < 0·05$: significantly different from the control group and IL-4 (Student's t-test). (b) Inhibition of the effecter phase of chronic hypersensitivity by IL-4DM, IL-4, and control plasmid DNA transfer. The ear swelling was measured 30 min after applying OX. The ear swelling in the IL-4DM groups was significantly suppressed compared with those in the IL-4 and control plasmid DNA groups. *Significant difference from the control by Student's t-test at $P < 0·05$.

Cytokine production from splenocytes

A suspension of 2×10^6 splenocytes were made in a solution of 200 μL RPMI-1640 medium (Nikken Bio Medical Laboratory, Kyoto, Japan) containing 10% fetal bovine serum (FBS; Biowest, Nuaillé, France), 50 UI penicillin, 50 μg mL^{-1} streptomycin, and 5 μg mL^{-1} soluble antimouse CD3 (BD Bioscience), and 10 μg mL^{-1} antimouse CD28 (BD Bioscience). Cells were dispensed in triplicate into 96-well flat-bottomed microplates (Sumitomo Bakelite, Tokyo, Japan). After incubation for 48 h at 37 °C in a humidified incubator (5% CO_2), culture supernatants were collected and analysed for IFN-γ (Quantikine; R&D Systems, Minneapolis, MN, U.S.A.) or IL-4 (Quantikine; R&D Systems) production with an ELISA according to the manufacturer's protocol.

Statistical analysis

Statistical analysis was performed using Student's t-test and Mann–Whitney U-test. Values are expressed as mean ± SEM. A 95% confidence limit was taken as significant ($P < 0.05$).

Result

Ear thickness with the treatment of IL-4DM, IL-4, or control plasmid

In the control group, the ear thickness increased from the beginning of the challenge, and increased gradually through the experiments (Fig. 2a). The agonistic IL-4 DNA treatment augmented increase of the ear thickness after day 16. In contrast, IL-4DM DNA treatment significantly suppressed increase of the ear thickness compared with that of control plasmid or IL-4DNA-treated mice.

Effects of IL-4DM on the oxazolone-induced acute-phase ear swelling

The ear swelling was also measured 30 min after OX application on day 35, and the difference between before and 30 min after application was calculated. IL-4DM DNA treatment suppressed the ear swelling significantly compared with that of the control DNA-injected group (Fig. 2b). However, IL-4DNA showed no suppressive effects.

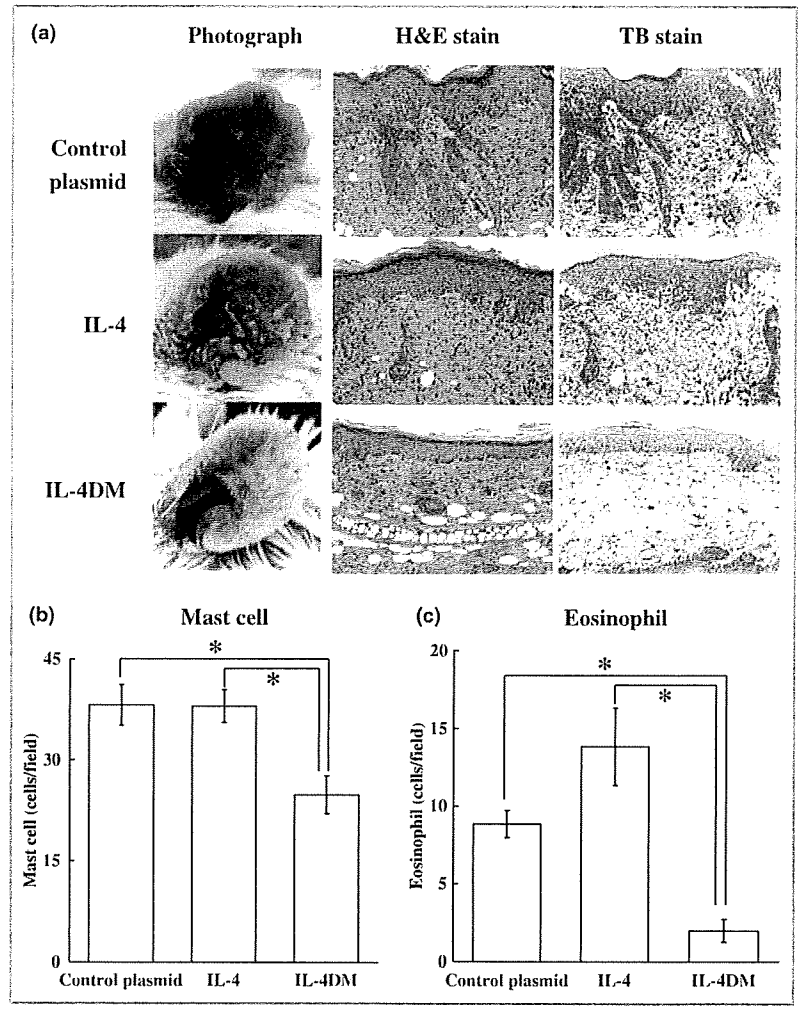

Fig 3. (a) Representative photographs and histological feature of oxazolone (OX)-treated skin lesion. OX-sensitized ear revealed hyperkeratosis, acanthosis, and parakeratosis in control and interleukin (IL)-4-treated mice. An increased number of infiltrating lymphocytes, macrophages and mast cells was observed in the skin lesions, all of which are typical histological findings observed in patients with atopic dermatitis. In contrast, acanthosis was clearly suppressed, and skin infiltration of granulocytes, eosinophils, and mast cells was decreased in the IL-4DM-treated mice as compared with control plasmid-treated mice (original magnification × 200). (b) The number of dermal mast cells was counted, and found to be decreased in the IL-4DM-treated mice. (c) The number of dermal eosinophils was also counted in 10 high power fields. The skin infiltration of eosinophils was significantly decreased in the IL-4DM-treated mice. Data are expressed as the mean ± SEM. *Significant difference by Student's t-test at $P < 0.05$.

Histological findings and mast cell counts in the inflamed skin

In control plasmid-treated mice and IL-4 DNA-treated mice, severe dermatitis was observed on the earlobe. A drastic decrease of inflammation was observed in IL-4DM DNA-treated mice (Fig. 3a). Histological examination on the OX-challenged ear skin revealed hyperkeratosis, acanthosis and parakeratosis in both of the control and IL-4-treated mice. An increased number of infiltrating lymphocytes, macrophages and mast cells was observed in the skin lesions in control DNA and IL-4 DNA-treated mice. These findings are comparable with those of AD skin lesions. In contrast, the acanthotic changes and infiltration of granulocytes, mast cells, and eosinophils were significantly suppressed in the IL-4DM DNA-treated mice compared with those of control DNA- or IL-4 DNA-treated mice (Fig. 3b,c). Interestingly, IL-4 DNA treatment increased eosinophil counts compared with control DNA treatment.

Plasma IgE and histamine levels

The total plasma IgE level was increased by repeated OX challenges (Fig. 4a). IL-4 DNA treatment showed no agonistic effects in the plasma IgE level; however, IL-4DM DNA treatment significantly suppressed the levels of plasma IgE. The plasma histamine level was also significantly increased in the control DNA- or IL-4 DNA-treated mice; however, IL-4DM DNA treatment significantly suppressed the plasma histamine levels (Fig. 4b).

Cytokine mRNA expression levels

To determine the effects of IL-4DM on cytokine production in the inflamed skin lesions, mRNA expression of Th1 and Th2 cytokines was analysed. The IFN-γ mRNA expression was significantly increased in IL-4DM DNA-treated mice ear compared with that of control DNA-treated samples (standardized by β-actin expression).

However, no remarkable difference in other cytokine mRNA expression was observed among three different DNA-treated samples (Fig. 5a,b).

Concentration of IFN-γ and IL-4 in splenocyte cell culture supernatants

To know the effects of IL-4DM DNA therapy in the systemic immune system, the concentration of IFN-γ in splenocyte cell culture supernatants was measured by ELISA. The IFN-γ level in the IL-4DM-treated samples was significantly higher than that in the control DNA- or IL-4 DNA-treated samples (Fig. 6a). We also measured the concentration of IL-4 in splenocyte cell culture supernatants by ELISA for mouse IL-4. The IL-4 level in the IL-4DM-treated samples was as high as the IL-4 DNA-treated samples. These were higher than that of the control DNA-treated samples (Fig. 6b).

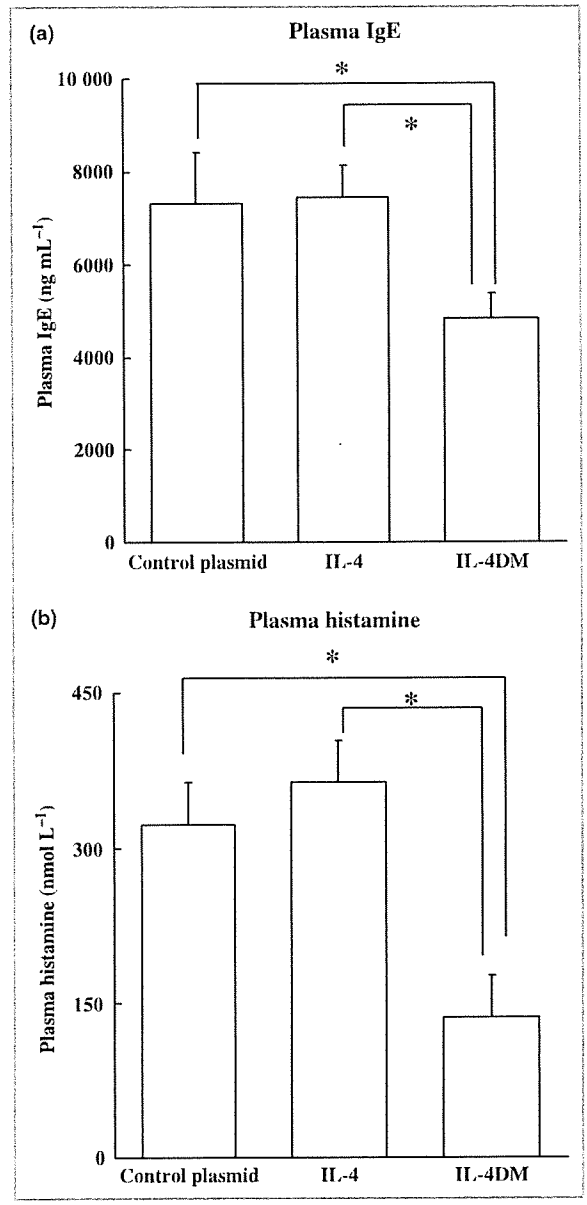

Fig 4. Plasma IgE and histamine levels. (a) Plasma IgE level was decreased in interleukin (IL)-4DM treated mice. (b) Inhibition of the production of plasma histamine was observed in IL-4DM DNA-treated mice. *Significant difference from the IL-4 and control by Mann–Whitney U-test at $P < 0{\cdot}05$.

Discussion

Several previous studies have shown that AD is a chronic dermatitis with a predominance of Th2 cytokines in the lesional skin,[27–29] and that Th2 cytokines play a critical role in the pathogenesis of dermatitis.[28] IL-4 is one of the Th2 cytokines that affects the function of different cell types including T cells, B cells, mast cells, monocytes/macrophages, endothelial cells, fibroblasts, dendritic cells, Langerhans cells

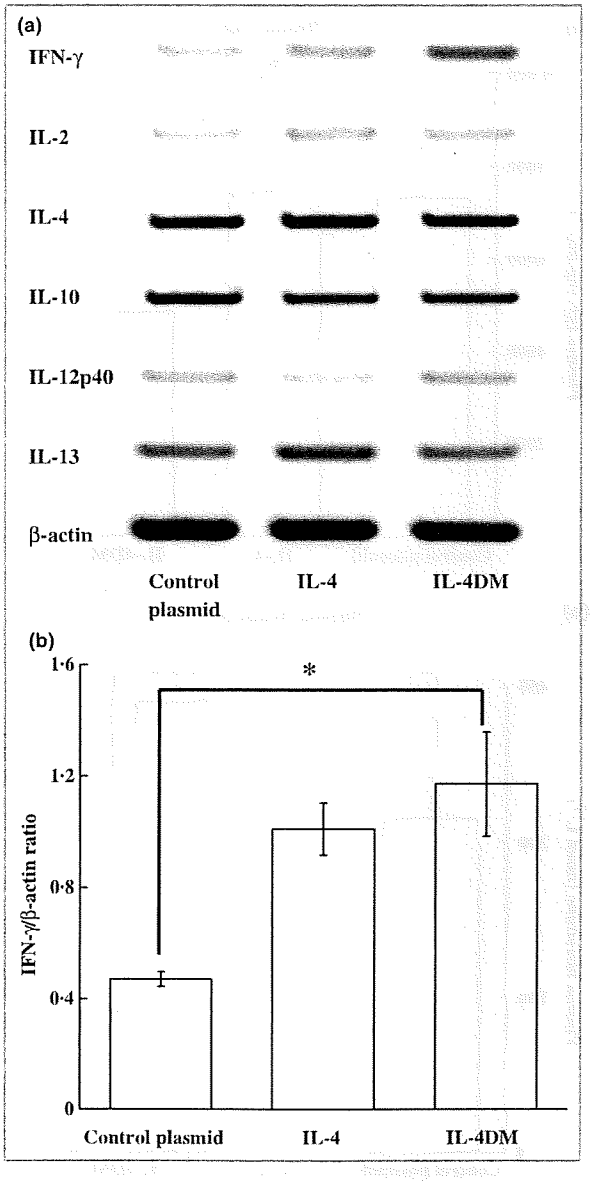

Fig 5. (a) Reverse-transcriptase polymerase chain reaction analysis of cytokine mRNA expression 6 h after oxazolone (OX)-sensitization. The cDNAs were amplified for respective cycles of six cytokines and β-actin, subjected to electrophoresis, and visualized with ethidium bromide. Representative results under optimal conditions are shown. Although almost all Th1 and Th2 cytokine levels were unchanged, mRNA expression for interferon (IFN)-γ was increased in IL-4DM-treated mice. (b) The level of mRNA expression of IFN-γ was expressed as the value relative to that for β-actin. The IFN-γ level in the IL-4DM group is significantly higher than that of control plasmid groups. *Significant difference from the control by Student's t-test at $P < 0{\cdot}05$.

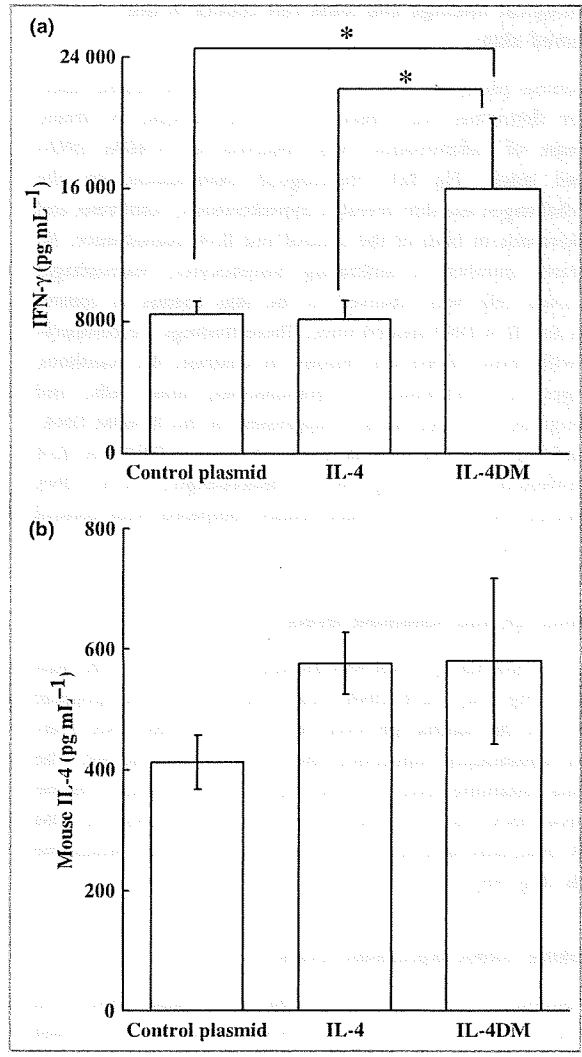

Fig 6. Cytokine production from splenocytes in chronic hypersensitivity mice. Interferon (IFN)-γ and interleukin (IL)-4 production from splenocytes was measured. (a) Actual IFN-γ protein production was increased in the IL-4DM-treated mice. (b) IL-4 levels did not reach the significance, but showed a tendency to increase in the IL-4 and IL-4DM mice. *Significant difference from the control by Mann–Whitney U-test at $P < 0{\cdot}05$.

and keratinocytes. Because of this broad-spectrum action, IL-4 is believed to play a crucial role in the pathogenesis of AD.[30,31] In the present study, we employed a contact hypersensitivity model by the repeated application of OX, which mimics the histological phenotype of AD in humans; this model also showed increased levels of Th2 cytokines in the lesional skin as reported by Kitagaki *et al.*[21]

Immunotherapy such as the direct blocking of Th2 responses with neutralizing antibody against Th2 cytokines, the soluble form of IL-4 receptor (IL-4R), or antagonistic IL-4 mutant proteins have been used for the treatment of asthma.[32–34] These proteins directly inhibit IL-4 binding thereby inhibiting host immune responses. A previous study by Nishikubo *et al.*[25] showed inhibition of immune responses by using IL-4 mutant protein for at least 50 weeks. However, results from these experimental animals have shown that the application of these trials to humans is difficult. Because the pharmacokinetic half-life of IL-4 mutant and sIL-4R protein

are very short in vivo (IL-4 mutant: $t_{1/2}$ = 0·83 h; sIL-4R: $t_{1/2}$ = 4·6 h),[35,36] huge amounts of these molecules are required in plasma to maintain a long period of inhibitory action on allergic inflammation. In fact, administration of these molecules was required many times in high doses from the sensitization to the challenge periods.[35–37] In the present study, we demonstrated a remarkable antagonistic effect of IL-4 mutant DNA applied in a form of vaccination, as a potent new type of immunogene therapy for AD. In previous studies in which gene therapy and DNA vaccines were used in combination with a cytokine gene for tumours or pathogens, effective immune responses to antigen were recognized even in the absence of detectable plasma levels of cytokines. Recently, we also reported that administration of plasmid DNA coding IL-4 cDNA completely inhibited the development of insulitis, which is one of the Th1-type autoimmune diseases, although no IL-4 was detected in plasma.[38] These results suggest that genes applied as a DNA vaccine express and supply products to the host continuously. To occupy the IL-4/IL-13 receptors, a continuous supply of IL-4DM is needed but not bolus application. Therefore, IL-4DM applied as a DNA vaccine might inhibit the allergic inflammation by persistent secretion of mutant IL-4 over a long period in a limited amount.

As we had expected, IL-4DM mitigated phenotypical and histological changes such as severe oedema, inflammatory cell infiltration and epidermal hyperplasia. IL-4DM also significantly decreased the number of dermal mast cells. IL-4 is known to be a potent activator of mast cells. Mast cells, which participate in the inflammatory cascade, serve as an abundant source of Th2 cytokines as well as inflammatory mediators.[39–41] Therefore, inhibition of mast cell activation is another possible mechanism through which IL-4DM ameliorates inflammatory responses in the present model of dermatitis. Eosinophil infiltration into the dermis has been well documented in AD.[42] In this study, an increased number of eosinophils was observed in contact hypersensitivity skin lesions, and was dramatically inhibited by IL-4DM treatment. Inhibition of cellular infiltration in IL-4DM mice may be due to suppression of IL-4-mediated immunological events such as a decreased expression of cellular adhesion molecules on endothelial cells.[43]

Injected IL-4DM and IL-4 DNA are trapped by monocytes/macrophages by phagocytosis. They may migrate to lymph nodes or spleen and show systemic effects. In fact, we could observe a high concentration of IL-4 in cultured splenocytes from IL-4DM DNA injected mice by ELISA. Unfortunately, there is no specific anti-IL-4DM antibody or anti-IL-4DM ELISA. The standard ELISA used in this study could not differentiate the natural mouse IL-4 and mutant IL-4 protein; these findings are consistent with the previous report.[25] The plasma IL-4 levels in the agonistic IL-4DNA-treated mice were consistent with those of the IL-4DM DNA-treated mice. Therefore, we speculate that exogenously applied IL-4DM DNAs were expressed the same as IL-4 DNAs, and showed systemic immunological effects.

IFN-γ production increased systemically and locally in mice treated with IL-4DM DNA. Repeated OX treatments cause expansion both of Th1 and Th2 cells. IL-4DM DNA therapy interfered with the development of the Th2 milieu. Subsequently, IFN-γ production and mRNA expression might become abundant locally and systemically.

Tissue-specific gene transfer could be achieved naturally and effectively through the cell specificity of virus receptors.[44] However, there may be a risk of vector toxicity through viral infection of host cells. Also, the limited size of transgenes is often a serious obstacle. Moreover, immune responses to viral vectors are also induced, and the effects of transgenes are eliminated by immune responses to the vectors. For human applications, the efficacy and safety of any delivery system for gene transfer are always of major concern. Nonviral approaches are advantageous in immunogene therapy. DNA vaccines are capable of inducing potent biological effects in a variety of experimental systems.[45] One of the characteristic features of DNA vaccines is their ability to induce long-lasting immunity. The animals that had been treated with IL-4DM DNA did not develop severe allergic inflammation even before or after antigen sensitization.

In the present study, we showed the beneficial effects of immunogene therapy with IL-4 mutant DNA in an experimental model for AD. An IL-4 mutant DNA vaccination is a potent new tool for the systemic treatment of AD.

Acknowledgments

Grants-in-Aid for Scientific Research and Grants-in-Aid for Core Research Evolutional Science and Technology.

References

1 Paul WE. Interleukin-4: a prototypic immunoregulatory lymphokine. Blood 1991; **77**:1859–70.
2 Mosmann TR, Sad S. The expanding universe of T-cell subsets: Th1, Th2 and more. Immunol Today 1996; **17**:138–46.
3 Romagnani S. The Th1/Th2 paradigm. Immunol Today 1997; **18**:263–6.
4 Zurawski G, de Vries JE. Interleukin 13, an interleukin 4-like cytokine that acts on monocytes and B cells, but not on T cells. Immunol Today 1994; **15**:19–26.
5 Tony HP, Shen BJ, Reusch P et al. Design of human interleukin-4 antagonists inhibiting interleukin-4-dependent and interleukin-13-dependent responses in T-cells and B-cells with high efficiency. Eur J Biochem 1994; **225**:659–65.
6 Smerz-Bertling C, Duschl A. Both interleukin 4 and interleukin 13 induce tyrosine phosphorylation of the 140-kDa subunit of the interleukin 4 receptor. J Biol Chem 1995; **270**:966–70.
7 Kruse N, Tony HP, Sebald W. Conversion of human interleukin-4 into a high affinity antagonist by a single amino acid replacement. EMBO J 1992; **11**:3237–44.
8 Kruse N, Shen BJ, Arnold S et al. Two distinct functional sites of human interleukin 4 are identified by variants impaired in either receptor binding or receptor activation. EMBO J 1993; **12**:5121–9.
9 Zurawski SM, Vega F Jr, Huyghe B et al. Receptors for interleukin-13 and interleukin-4 are complex and share a novel component that functions in signal transduction. EMBO J 1993; **12**:2663–70.

10 Aversa G, Punnonen J, Cocks BG *et al.* An interleukin 4 (IL-4) mutant protein inhibits both IL-4 or IL-13-induced human immunoglobulin G4 (IgG4) and IgE synthesis and B cell proliferation: support for a common component shared by IL-4 and IL-13 receptors. *J Exp Med* 1993; **178**:2213–18.

11 Zurawski SM, Chomarat P, Djossou O *et al.* The primary binding subunit of the human interleukin-4 receptor is also a component of the interleukin-13 receptor. *J Biol Chem* 1995; **270**:13869–78.

12 Konig B, Fischer A, Konig W. Modulation of cell-bound and soluble CD23, spontaneous and ongoing IgE synthesis of human peripheral blood mononuclear cells by soluble IL-4 receptors and the partial antagonistic IL-4 mutant protein IL-4 (Y124D). *Immunology* 1995; **85**:604–10.

13 Carballido JM, Schols D, Namikawa R *et al.* IL-4 induces human B cell maturation and IgE synthesis in SCID-hu mice. Inhibition of ongoing IgE production by *in vivo* treatment with an IL-4/IL-13 receptor antagonist. *J Immunol* 1995; **155**:4162–70.

14 Carballido JM, Aversa G, Schols D *et al.* Inhibition of human IgE synthesis *in vitro* and in SCID-hu mice by an interleukin-4 receptor antagonist. *Int Arch Allergy Immunol* 1995; **107**:304–7.

15 Schnyder B, Lugli S, Feng N *et al.* Interleukin-4 (IL-4) and IL-13 bind to a shared heterodimeric complex on endothelial cells mediating vascular cell adhesion molecule-1 induction in the absence of the common gamma chain. *Blood* 1996; **87**:4286–95.

16 Sornasse T, Larenas PV, Davis KA *et al.* Differentiation and stability of T helper 1 and 2 cells derived from naive human neonatal CD4+ T cells, analyzed at the single-cell level. *J Exp Med* 1996; **184**:473–83.

17 Vannier E, de Waal Malefyt R, Salazar-Montes A *et al.* Interleukin-13 (IL-13) induces IL-1 receptor antagonist gene expression and protein synthesis in peripheral blood mononuclear cells: inhibition by an IL-4 mutant protein. *Blood* 1996; **87**:3307–15.

18 Schnarr B, Ezernieks J, Sebald W *et al.* IL-4 receptor complexes containing or lacking the gamma C chain are inhibited by an overlapping set of antagonistic IL-4 mutant proteins. *Int Immunol* 1997; **9**:861–8.

19 Grunewald SM, Kunzmann S, Schnarr B *et al.* A murine interleukin-4 antagonistic mutant protein completely inhibits interleukin-4-induced cell proliferation, differentiation, and signal transduction. *J Biol Chem* 1997; **272**:1480–3.

20 Andersson A, Grunewald SM, Duschl A *et al.* Mouse macrophage development in the absence of the common gamma chain: defining receptor complexes responsible for IL-4 and IL-13 signaling. *Eur J Immunol* 1997; **27**:1762–8.

21 Kitagaki H, Fujisawa S, Watanabe K *et al.* Immediate-type hypersensitivity response followed by a late reaction is induced by repeated epicutaneous application of contact sensitizing agents in mice. *J Invest Dermatol* 1995; **105**:749–55.

22 Kitagaki H, Kimishima M, Teraki Y *et al.* Distinct *in vivo* and *in vitro* cytokine profiles of draining lymph node cells in acute and chronic phases of contact hypersensitivity: importance of a type 2 cytokine-rich cutaneous milieu for the development of an early-type response in the chronic phase. *J Immunol* 1999; **163**:1265–73.

23 Mori H, Yamanaka K, Matsuo K *et al.* Administration of Ag85B showed therapeutic effects to Th2-type cytokine-mediated acute phase atopic dermatitis by inducing regulatory T cells. *Arch Dermatol Res* 2009; **301**:151–7.

24 Kopf M, Le Gros G, Bachmann M *et al.* Disruption of the murine IL-4 gene blocks Th2 cytokine responses. *Nature* 1993; **362**:245–8.

25 Nishikubo K, Murata Y, Tamaki S *et al.* A single administration of interleukin-4 antagonistic mutant DNA inhibits allergic airway inflammation in a mouse model of asthma. *Gene Ther* 2003; **10**:2119–25.

26 Overbergh L, Valckx D, Waer M *et al.* Quantification of murine cytokine mRNAs using real time quantitative reverse transcriptase PCR. *Cytokine* 1999; **11**:305–12.

27 Kay AB, Ying S, Varney V *et al.* Messenger RNA expression of the cytokine gene cluster, interleukin 3 (IL-3), IL-4, IL-5, and granulocyte/macrophage colony-stimulating factor, in allergen-induced late-phase cutaneous reactions in atopic subjects. *J Exp Med* 1991; **173**:775–8.

28 Herz U, Bunikowski R, Renz H. Role of T cells in atopic dermatitis. New aspects on the dynamics of cytokine production and the contribution of bacterial superantigens. *Int Arch Allergy Immunol* 1998; **115**:179–90.

29 Akdis CA, Akdis M, Trautmann A *et al.* Immune regulation in atopic dermatitis. *Curr Opin Immunol* 2000; **12**:641–6.

30 Ricci M, Matucci A, Rossi O. IL-4 as a key factor influencing the development of allergen-specific Th2-like cells in atopic individuals. *J Investig Allergol Clin Immunol* 1997; **7**:144–50.

31 Elbe-Burger A, Egyed A, Olt S *et al.* Overexpression of IL-4 alters the homeostasis in the skin. *J Invest Dermatol* 2002; **118**:767–78.

32 Zhou CY, Crocker IC, Koenig G *et al.* Anti-interleukin-4 inhibits immunoglobulin E production in a murine model of atopic asthma. *J Asthma* 1997; **34**:195–201.

33 Tomaki M, Zhao LL, Lundahl J *et al.* Eosinophilopoiesis in a murine model of allergic airway eosinophilia: involvement of bone marrow IL-5 and IL-5 receptor alpha. *J Immunol* 2000; **165**:4040–50.

34 Bost KL, Holton RH, Cain TK *et al.* *In vivo* treatment with anti-interleukin-13 antibodies significantly reduces the humoral immune response against an oral immunogen in mice. *Immunology* 1996; **87**:633–41.

35 Henderson WR Jr, Chi EY, Maliszewski CR. Soluble IL-4 receptor inhibits airway inflammation following allergen challenge in a mouse model of asthma. *J Immunol* 2000; **164**:1086–95.

36 Tomkinson A, Duez C, Cieslewicz G *et al.* A murine IL-4 receptor antagonist that inhibits IL-4- and IL-13-induced responses prevents antigen-induced airway eosinophilia and airway hyperresponsiveness. *J Immunol* 2001; **166**:5792–800.

37 Grunewald SM, Werthmann A, Schnarr B *et al.* An antagonistic IL-4 mutant prevents type I allergy in the mouse: inhibition of the IL-4/IL-13 receptor system completely abrogates humoral immune response to allergen and development of allergic symptoms *in vivo*. *J Immunol* 1998; **160**:4004–9.

38 Hayashi T, Yasutomi Y, Hasegawa K *et al.* Interleukin-4-expressing plasmid DNA inhibits reovirus type-2-triggered autoimmune insulitis in DBA/1 J suckling mice. *Int J Exp Pathol* 2003; **84**:101–6.

39 Ruzicka T, Gluck S. Cutaneous histamine levels and histamine releasability from the skin in atopic dermatitis and hyper-IgE-syndrome. *Arch Dermatol Res* 1983; **275**:41–4.

40 Horsmanheimo L, Harvima IT, Jarvikallio A *et al.* Mast cells are one major source of interleukin-4 in atopic dermatitis. *Br J Dermatol* 1994; **131**:348–53.

41 Gibbs BF, Wierecky J, Welker P *et al.* Human skin mast cells rapidly release preformed and newly generated TNF-alpha and IL-8 following stimulation with anti-IgE and other secretagogues. *Exp Dermatol* 2001; **10**:312–20.

42 Leung DY. Atopic dermatitis: immunobiology and treatment with immune modulators. *Clin Exp Immunol* 1997; **107** (Suppl. 1):25–30.

43 Schleimer RP, Sterbinsky SA, Kaiser J *et al.* IL-4 induces adherence of human eosinophils and basophils but not neutrophils to endothelium. Association with expression of VCAM-1. *J Immunol* 1992; **148**:1086–92.

44 Mistry AR, Falciola L, Monaco L *et al.* Recombinant HMG1 protein produced in Pichia pastoris: a nonviral gene delivery agent. *BioTechniques* 1997; **22**:718–29.

45 Gurunathan S, Klinman DM, Seder RA. DNA vaccines: immunology, application, and optimization. *Annu Rev Immunol* 2000; **18**:927–74.

Parasitol Res (2009) 105:929–937
DOI 10.1007/s00436-009-1480-3

ORIGINAL PAPER

DNA characterization of simian *Entamoeba histolytica*-like strains to differentiate them from *Entamoeba histolytica*

Jun-ichiro Takano · Hiroshi Tachibana · Miyoko Kato · Toyoko Narita · Tetsuo Yanagi · Yasuhiro Yasutomi · Koji Fujimoto

Received: 27 March 2009 / Accepted: 8 May 2009 / Published online: 27 May 2009

Abstract Two simian *Entamoeba histolytica*-like strains, EHMfas1 and P19-061405, have been suggested to represent a new species based on genetic characterization. Sequence analyses of the hexokinase, glucose phosphate isomerase, and phosphoglucomutase genes supported the previous findings of isoenzyme analyses demonstrating a new zymodeme pattern. Phylogenetic studies of 18S rDNA, 5.8S rDNA, the chaperonin 60 gene, and the pyridine nucleotide transhydrogenase gene showed original clusters of simian *E. histolytica*-like strains below or near *E. histolytica*, respectively. Comparative studies of the chitinase and the serine-rich *E. histolytica* protein genes and locus 1–2 region revealed that most mutated units were shared among the simian *E. histolytica*-like strains. The similarities of each of the repeating units within the simian *E. histolytica*-like strains or *E. histolytica* and the differences of those between the both might be generated by concerted evolution. Our results indicate that EHMfas1 and P19-061405 should be considered to be the same species, despite that they were isolated from different monkey species and different habitats. Simian *E. histolytica*-like amebas may be endemic to macaque monkeys, as a counterpart to *E. histolytica* in humans, and should be differentiated from *E. histolytica* by the revival name *Entamoeba nuttalli*, as proposed for P19-061405.

J.-i. Takano (✉) · M. Kato · T. Narita · K. Fujimoto
The Corporation for Production and Research
of Laboratory Primates,
1-1 Hachimandai,
Tsukuba, Ibaraki 305-0843, Japan
e-mail: takano@primate.or.jp

H. Tachibana
Department of Infectious Diseases,
Tokai University School of Medicine,
143 Shimokasuya,
Isehara, Kanagawa 259-1193, Japan

T. Yanagi
Animal Research Center for Tropical Infections,
Institute of Tropical Medicine, Nagasaki University,
1-12-4 Sakamoto,
Nagasaki, Nagasaki 852-8523, Japan

Y. Yasutomi
Tsukuba Primate Research Center,
National Institute of Biomedical Innovation,
1-1 Hachimandai,
Tsukuba, Ibaraki 305-0843, Japan

Introduction

Entamoeba histolytica causes amoebic colitis and liver abscess, and amoebiasis is one of the most important parasitic diseases in humans. In non-human primates, several cases of *E. histolytica* or *E. histolytica*-like organism infections have been identified by isoenzyme analysis, monoclonal antibody test, or PCR (Tachibana et al. 1990; Verweij et al. 2003; Takano et al. 2005; Tachibana et al. 2007; Suzuki et al. 2007). One of the simian *E. histolytica*-like strains, EHMfas1, has been isolated from a healthy cynomolgus monkey (*Macaca fascicularis*) and identified using species-specific PCR for *E. histolytica* and antigen-capture ELISA (Takano et al. 2005). Another simian *E. histolytica*-like strain, P19-061405, has been isolated from a rhesus monkey (*Macaca mulatta*). Furthermore, the virulence of P19-061405 has also been confirmed by experimental infection of hamsters (Tachibana et al. 2007).

These two simian *E. histolytica*-like strains were suggested to be a new species, because EHMfas1 exhibits differences in the 16S-like small subunit ribosomal RNA

(18S rDNA), chitinase and SREHP genes, and P19-061405 exhibits differences in several DNA sequences, including the 18S rDNA and SREHP genes (Takano et al. 2007; Tachibana et al. 2007). It has been proposed that P19-061405 should be distinguished from *E. histolytica* by revival of the name *Entamoeba nuttalli* (Castellani 1908) that was the first reported *E. histolytica*-like species found in a liver abscess of a monkey (Tachibana et al. 2007). Isoenzyme analyses of these two simian *E. histolytica*-like strains have demonstrated a new and similar zymodeme pattern.

In this study, we compared these two simian *E. histolytica*-like strains based on DNA loci that were used for isoenzyme analysis, phylogenetic investigation, and genotyping to determine the similarity between the simian *E. histolytica*-like strains and the differences between simian *E. histolytica*-like amebas and *E. histolytica*.

Materials and methods

Simian *E. histolytica*-like strains

Trophozoites of the EHMfas1 strain were cultured monoxenically with *Crithidia fasciculata* and axenically in BI-S-33 medium supplemented with 15% adult bovine serum at 37°C (Diamond et al. 1978) and then cloned by limiting dilution, followed by examination using microscopy. Trophozoites of the cloned P19-061405 strain were also axenically cultured in BI-S-33 medium (Tachibana et al. 2007).

Hepatic inoculation of hamsters

Hamsters were inoculated with trophozoites of the EHMfas1 that had been cultured monoxenically with *C. fasciculata* as described by Tachibana et al. (2007).

DNA preparation and sequencing

Total genomic DNA from each cloned trophozoite was extracted using a QIAamp DNA Stool Mini Kit (Qiagen) or a DNeasy tissue kit (Qiagen) according to the manufacturer's instructions.

The genomic DNA from cloned trophozoites was amplified using the primers listed in Table 1. PCR was conducted in a 50 μl reaction mixture containing 2 μl of extracted DNA and 0.1 μg/μl bovine serum albumin using PrimeSTAR Max DNA polymerase (Takara). A total of 35 cycles of PCR were performed, as follows: denaturation at 98°C for 10 s, annealing at 62°C (for pyridine nucleotide transhydrogenase (PNT)) or 56°C (for other genes) for 5 s, and extension at 72°C for 15 s.

Amplified genes for hexokinase (HXK), glucose-6-phosphate isomerase (GPI), and phosphoglucomutase (PGM) from EHMfas1 and chaperonin 60 (Cpn60) were cloned from P19-061405 using a Zero Blunt TOPO PCR cloning kit for sequencing (Invitrogen). Each clone was subjected to sequencing using a BigDye Terminator v3.1 Cycle Sequencing Kit (Applied Biosystems) on an ABI PRISM 3100-Avant Genetic Analyzer (Applied Biosystems), according to the manufacturer's instructions. PCR products for 5.8S rDNA with internal-transcribed spacer (ITS) 1 and ITS 2, Cpn60, and PNT, locus 1–2 from EHMfas1 and PNT, and chitinase and locus 1–2 from P19-061504 were sequenced directly. Sequence data were analyzed using DNASIS Pro ver. 2.08 (Hitachi software). The GenBank accession numbers of the sequences used for comparison with each gene are shown in Figs. 1, 2, 3, and 4.

Phylogenetic analysis

Analysis and multiple alignments of DNA sequences of 18S rDNA, 5.8S rDNA with ITS 1 and ITS 2, Cpn60, and PNT were performed with ClustalX (Thompson et al. 1997), and the phylogenetic trees were constructed using the neighbor-joining method (Saitou and Nei 1987).

Nucleotide sequence accession numbers

The nucleotide sequence data reported here have been submitted to the GenBank/EMBL/DDBJ databases under accession numbers AB454548 to AB454559 and AB480745.

Results

Virulency of EHMfas1 in hamster

EHMfas1 was monoxenically cultured with *C. fasciculata* and inoculated into the livers of hamsters. Liver abscesses were observed in all hamsters at 7 days after inoculation. The presence of trophozoites in the peripheral regions of abscesses in the livers was confirmed in PAS stained tissue slides. No abscesses were observed in the control hamsters, inoculated with *C. fasciculata* alone.

Analysis of zymodeme-related genes

Two HXK genes of EHMfas1 were amplified from the cloned EHMfas1 trophozoites and sequenced after molecular cloning. The calculated molecular masses and isoelectric points (p*I*) were 49.7 kDa and 5.38 in HXK 1 and 49.4 kDa and 4.99 in HXK 2. The deduced amino-acid sequences were compared with those of P19-061405

Table 1 Primers used in this study

Locus	Direction (name of primer)	Sequence (5′-3′)	Reference
HXK	S	ATG CAA GAA ATC ATT GAT CAA TTT	Tachibana et al. 2007
HXK1	AS	TTA GTG TTT ACA TGC AAC AGC A	
HXK2	AS	TTA TTG TTT GCA TGC AAC AGC A	
GPI	S	ATG TTA CCA ACT CTT CCT GAA T	Tachibana et al. 2007
	AS	TTA GTT TTT TCT CAT ATC TTT AAC A	
PGM	S (PGMoutS)	TCG TTG AAC CAG ATC AGT GC	Genome database region on scaffold 00005[a]
	AS (PGMoutAS)	AAG CTT CTC TGG ATG GTG TTG	
ITS1, 5.8S	S (P1)	AGG TGA ACC TGC GGA AGG ATC ATT A	Som et al. 2000
ITS2	AS (P2)	TCA TTC GCC ATT ACT TAA GAA ATC ATT GTT	
Cpn60	S (CpnOf1)	GTT GAA CTT TTC ATA AGG TTG TTT GA	Genome database region on scaffold 00015[a]
	AS (CpnOr1)	CAA AAA TGG GCA GAT GAA CA	
PNT	S (PNT-A)	GTA GGA CTT GCA GCA GTA TT	Bakatselou et al. 2003
	AS (PNT-B)	GGT AAT CTT CCT GCA ACT GG	
Chitinase	S	GGA ACA CCA GGT AAA TGT ATA	Ghosh et al. 2000
	AS	TCT GTA TTG TGC CCA ATT	
Locus 1–2	S (R1)	CTG GTT AGT ATC TTC GCC TGT	Zaki et al. 2002
	AS (R2)	CTT ACA CCC CCA TTA ACA AT	

S sense, *AS* anti-sense

[a] Present study

(GenBank accession numbers: AB282663 for HXK 1 and AB282664 for HXK 2). Glu^{13} and Asn^{32} in HXK 1 of P19-061405 were changed to Gly and Asp, respectively, in HXK 1 of EHMfas1. HXK 2 of EHMfas1was identical to that of P19-061405. The p*I*s for HXK 1 and HXK 2 of EHMfas1 were consistent with those of P19-061405 (Tachibana et al. 2007).

The GPI gene of EHMfas1 was also amplified and sequenced after molecular cloning, and only one GPI gene was obtained from 16 clones. The calculated molecular mass and p*I* for GPI of EHMfas1, 61.4 kDa and 6.60, were also consistent with those of P19-061405. In the deduced amino-acid sequence, Val^{232} in GPI 1 of P19-061405 (GenBank accession number: AB282665) was changed to Ile, and Val^{330} in the GPI 2 of P19-061405 (GenBank accession number: AB282666) was changed to Ala in EHMfas1.

One PGM gene from EHMfas1 was detected in clones from EHMfas1. The calculated molecular mass and p*I* for PGM were 60.8 kDa and 5.99, respectively. In the deduced amino-acid sequence of PGM from EHMfas1, there were four and 13 differences compared with *E. histolytica* (GenBank accession number: Y14444) and *Entamoeba dispar* (GenBank accession number: Y14445), respectively. Although the isoenzyme pattern of PGM in EHMfas1 was identical to *E. dispar*, the amino-acid sequences of PGM in EHMfas1 were more similar to *E. histolytica* than *E. dispar*.

Analyses and phylogenic studies of ribosomal RNA genes and mitosome genes

Comparison of the 18S rDNA sequences reported for EHMfas1 (Takano et al. 2007) and P19-061405 (Tachibana et al. 2007) showed a difference of 0.1% (two of 1,945). A reconstructed phylogenetic tree showed the original cluster of simian *E. histolytica*-like strains beside the *E. histolytica* branch (Fig. 1a). The 5.8S rDNA, with ITS 1 and 2 regions of EHMfas1, was sequenced directly. Comparison of this region of EHMfas1 and P19-061405 (Tachibana et al. 2007) showed no differences throughout the length. The constructed phylogenetic tree of this region also showed that the simian isolates were located beside the *E. histolytica* branch (Fig. 1b). The Cpn60 and PNT genes of EHMfas1 and P19-061405 were directly sequenced. Although DNAs were extracted from cloned trophozoites, obvious mixed sequences were confirmed by direct sequencing of Cpn60 gene from P19-061405. The Cpn60 gene from P19-061405 was cloned, and we obtained two Cpn60 gene alleles from six clones. In the nucleotide sequence of Cpn60 from EHMfas1, five and four differences were present compared with P19-061405 alleles 1 and 2, respectively. In the deduced amino-acid sequence, all Cpn60 from EHMfas1 and P19-061405 were consistent with *E. histolytica*. The phylogenetic relationship of the Cpn60 genes among *Entamoeba* species was also reconstructed (Fig. 1c). In

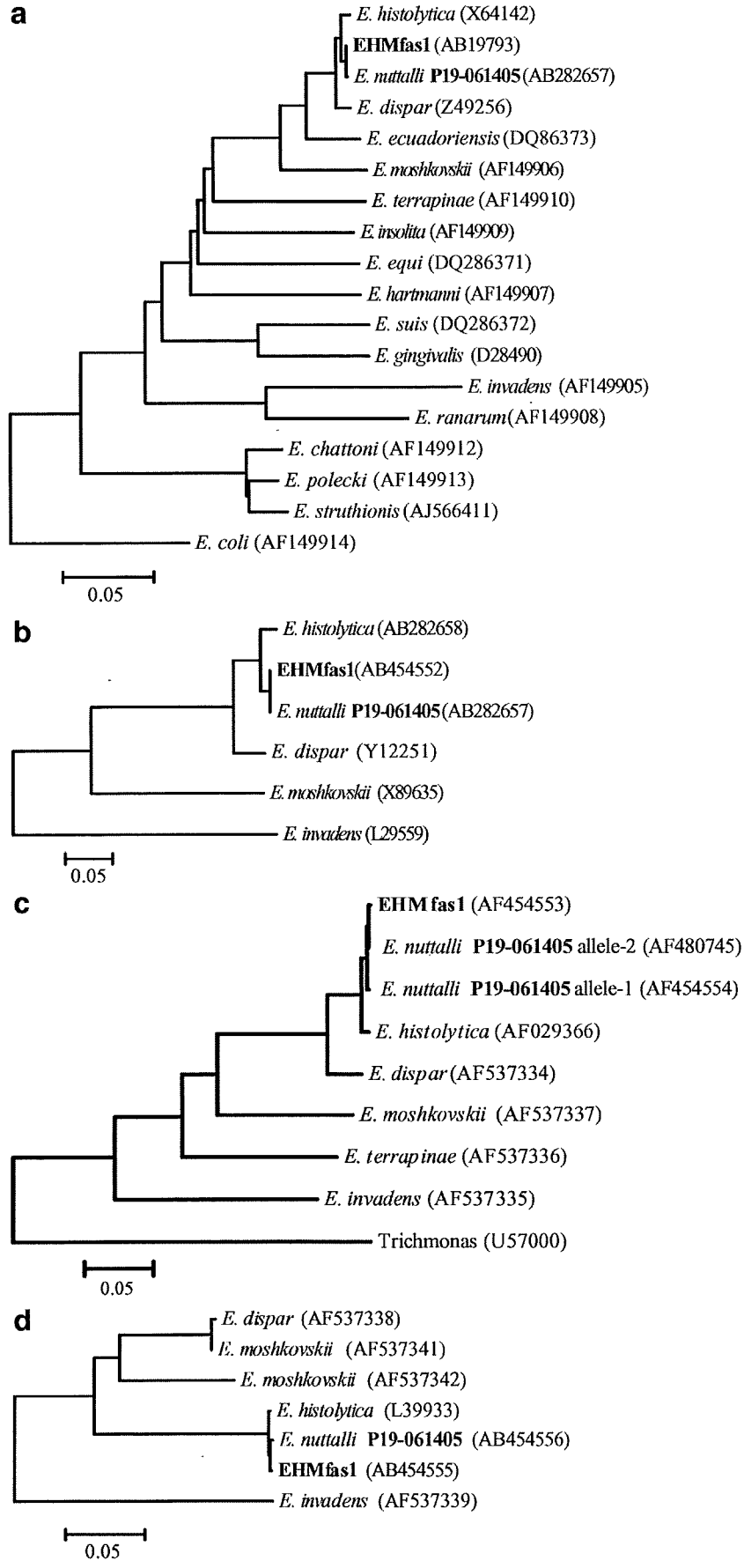

Fig. 1 Phylogenetic relationships among simian *E. histolytica*-like strains and other *Entamoeba* species. 18S rDNA sequences (**a**), 5.8S rDNA with ITS1 and ITS2 sequences (**b**), the Cpn60 gene sequences (**c**), and the PNT gene sequences (**d**). Branch lengths are proportional to estimated number of substitutions per site, which represent the evolutional distance

the reconstructed phylogenetic tree of the Cpn60 genes, the cluster of simian *E. histolytica*-like strains was located under the *E. histolytica* branch. PNT gene sequences were also compared between EHMfas1 and P19-061405, and a difference of 0.23% (one of 432) was evident. *E. histolytica*, EHMfas1 and P19-061405, was categorized in the same cluster (Fig. 1d).

Comparison of polymorphic loci: the chitinase gene, SREHP gene, and locus 1–2

The chitinase gene of P19-061405 was directly sequenced and compared with the reported sequences of EHMfas1, KU3 (genotype A) and KU15 (genotype D) of *E. histolytica* (Fig. 2; de la Vega et al. 1997; Ghosh et al. 2000; Haghighi et al. 2002, 2003). Each unit of the nucleotide and deduced amino-acid sequences was tentatively given a number, as in a previous study (Takano et al. 2007). All known EHMfas1-specific units, CN3, CN5, CN7, and CN3′C2, were also observed in P19-061405; however, the combination pattern of the repeating unit was different. Although P19-061405 was not classified into any known genotype, based on the nucleotide sequence, it was classified into genotype D based on the deduced amino-acid sequence in the polymorphic region.

Many SREHP genes of *E. histolytica* have been sequenced for genotyping (Li et al. 1992; Clark and Diamond 1993; Kohler and Tannich 1993; Stanley et al. 1990; Ayeh-Kumi et al. 2001; Haghighi et al. 2002, 2003). The reported SREHP gene sequences of EHMfas1, P19-061405 and *E. histolytica* KU27 (genotype I), were compared (Fig. 3). Each unit of the nucleotide and deduced amino-acid sequences was tentatively given a number, as in a previous study (Takano et al. 2007). All known EHMfas1-specific units, SN2, SN5, SN9, SN17, SN20, and SN3′C2, were also observed in P19-061405, but the combination pattern was different. The SN16 and DEE insertion, i.e., the second EHMfas1-specific insertion, were not observed in P19-061405. The nucleotide and deduced amino-acid sequences of P19-061405 were not classified into any of the known genotypes.

Locus 1–2 (also known as a non-coding short tandem repeat, D-A; Ali et al. 2005) of EHMfas1 and P19-061405 was directly sequenced and compared with the reported genotypes of *E. histolytica* (Zaki and Clark 2001; Haghighi et al. 2002, 2003). A number was tentatively assigned to each unit of the nucleotide sequences (Fig. 4). The nucleotide sequences of locus 1–2 were constructed from combinations of the 5′-conserved region, an 8 bp-repeating polymorphic region (8L1, 8L2, 8L3, and 8L4), intra-conserved region 1 (CL1, CL2, CL3, CL4, CL5,

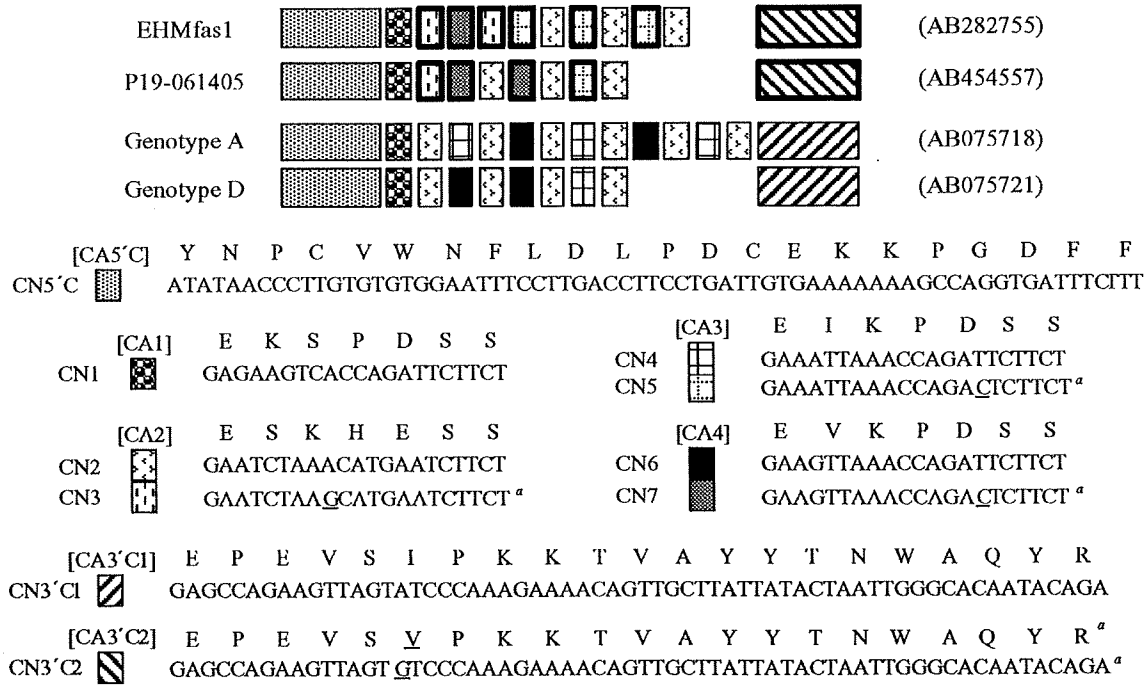

Fig. 2 Schematic representation of polymorphism in the repeat-containing region of the chitinase gene among simian *E. histolytica*-like strains and genotype A and D of *E. histolytica*. Nucleotide sequences pattern was shown. Each of nucleotide and deduced amino-acid sequences of unit was tentatively given a number. Nucleotide and deduced amino-acid sequences of these units are also shown. *Enclosed units with bold line* were simian *E. histolytica*-like strain-specific units. Simian *E. histolytica*-like strain-specific mutations in nucleotide and deduced amino-acid sequences are *underlined*. *a* Simian *E. histolytica*-like strain-specific unit sequences

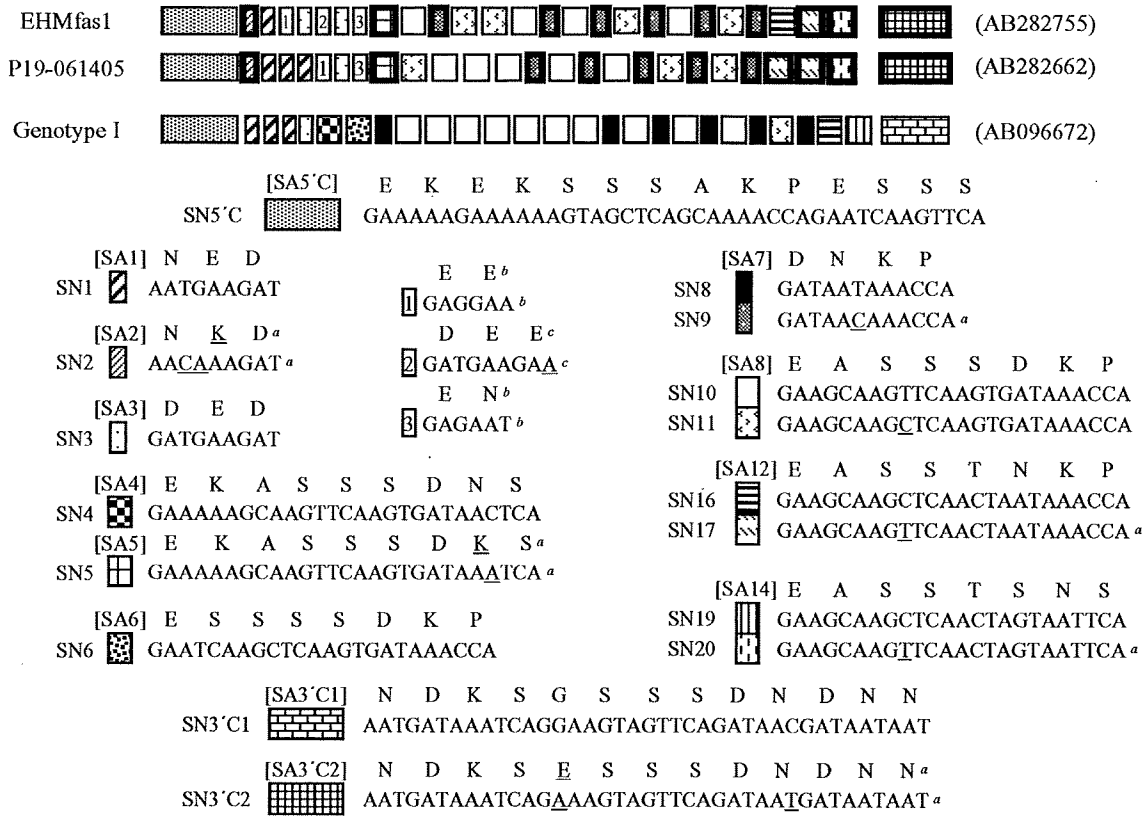

Fig. 3 Schematic representation of polymorphism in the repeat-containing region of the SREHP gene among simian *E. histolytica*-like strains and genotype I of *E. histolytica*. Nucleotide sequences pattern was shown. Each nucleotide and deduced amino-acid sequence of unit was tentatively given a number. Nucleotide and deduced amino-acid sequences of these units are also shown. *Enclosed units with bold line* were simian *E. histolytica*-like strain-specific units. Simian *E. histolytica*-like strain-specific mutations in nucleotide and deduced amino-acid sequences are *underlined*. *a* Simian *E. histolytica*-like strain-specific unit sequences. *b* Simian *E. histolytica*-like strain-specific block insertions. *c* EHMfas1-specific block insertion

CL6, and CL7), a 9-bp-repeating polymorphic region (9L1, 9L2, 9L3, 9L4, 9L5, and 9L6), intra-conserved region 2 (CL6, CL9, CL10, and CL11), a 12-bp-repeating polymorphic region (12L1, 12L2, 12L3, and 12L4), and the 3′-conserved region. The 8L1, 8L3, CL1, CL5, CL6, 9L1, 9L2, 9L4, and 12L3 units were common to simian *E. histolytica*-like strains and *E. histolytica*. On the other hand, 8L4, CL2, CL4, 9L3, 9L5, CL11, 12L2, and 12L4, were simian *E. histolytica*-like strain-specific mutated units. These mutated units corresponded to the 8L3, CL1, CL3, 9L2, 9L4, CL10, 12L1, and 12L3 units, with a single-nucleotide substitution in each unit, respectively. The CL8 was also a simian *E. histolytica*-like strain-specific unit that corresponded to CL7 with a four-nucleotide deletion (CCCT). Most units observed in *E. histolytica* were also observed in simian *E. histolytica*-like strains; however, all 12L1 were changed to 12L2 in the simian *E. histolytica*-like strains, and the CL9 was missing in the simian *E. histolytica*-like strains. Furthermore, 8L2 was observed only in EHMfas1 and corresponded to 8L1 with a double-nucleotide substitution.

Discussion

In this study, genetic similarities between EHMfas1 and P19-061405 and differences between simian *E. histolytica*-like strains and *E. histolytica* were revealed. EHMfas1 was also a virulent strain as P19-061405. The similar zymodeme patterns of EHMfas1 and P19-061405 have not been classified into any known patterns (Takano et al. 2007; Tachibana et al. 2007). Although some deduced amino acids were changed, the genetic similarities of HXK, GPI, and PGM supported the results of the isoenzyme analyses. HXK, GPI, and PGM of the simian *E. histolytica*-like strains were obviously more similar to *E. histolytica* than *E. dispar*. It is considered that EHMfas1 and P19-061405 are the same species, despite the fact that these strains were isolated from different host monkey species and a different habitat. Thus, simian *E. histolytica*-like amebas likely naturally infect macaques as a counterpart to *E. histolytica* in human.

Phylogenetic studies also indicated that EHMfas1 and P19-061405 are the same species and are closely related to *E. histolytica*. Nucleotide sequences of the 18S rDNA

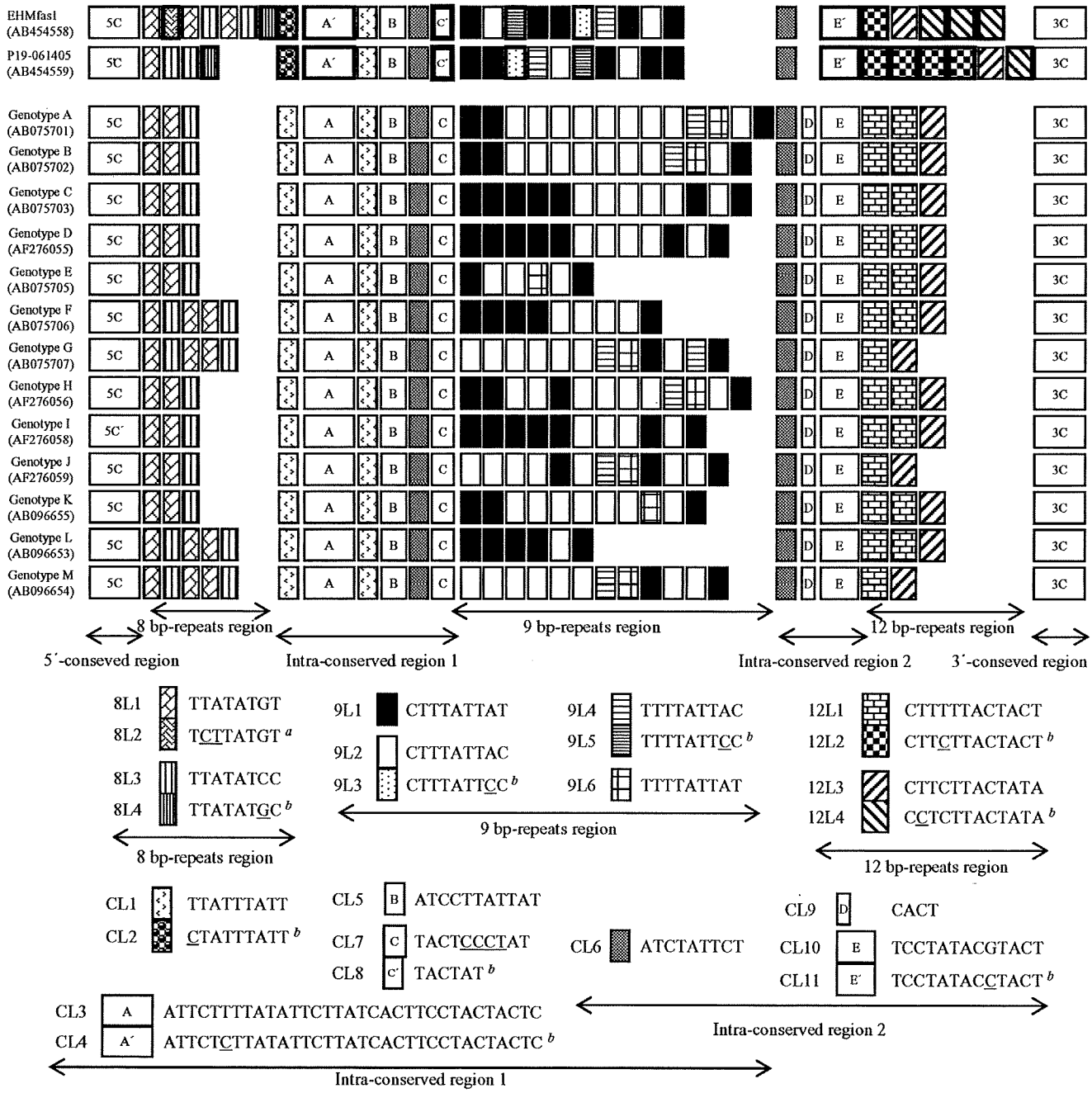

Fig. 4 Schematic representation of polymorphism in the repeat-containing region of the locus 1–2 region among simian *E. histolytica*-like strains and available *E. histolytica*. Nucleotide sequences pattern was shown. Each nucleotide sequence of unit was tentatively given a number. Nucleotide sequences of these units are also shown. *Enclosed units with bold line* were EHMfas1-specific or simian *E. histolytica*-like strain-specific units. EHMfas1-specific or simian *E. histolytica*-like strain-specific mutations in nucleotide sequences are *underlined*. Simian *E. histolytica*-like strain-specific deletion from human isolates is underlined at comparative sequence. *a* EHMfas1-specific unit sequence. *b* Simian *E. histolytica*-like strain-specific unit sequences

and 5.8S rDNA with ITS 1 and ITS 2 and Cpn60 and PNT genes of EHMfas1 and P19-061405 have been used for previous phylogenetic studies of the genus *Entamoeba* (Clark and Diamond 1997; Silberman et al. 1999; Som et al. 2000; Bakatselou et al. 2003; Clark et al. 2006). All phylogenetic studies indicated that EHMfas1 and P19-061405 generated an original cluster beside or under *E. histolytica*, including the PNT gene, which is known to contribute to an anomalous-shaped phylogenetic tree (Bakatselou et al. 2003).

Comparisons of polymorphic loci used for genotyping revealed notable differences from *E. histolytica* and

similarities between simian *E. histolytica*-like strains in sequence variation of the constructing units (Figs. 2, 3, and 4). The chitinase genes, the SREHP genes, and the locus 1–2 sequences of *E. histolytica* have been categorized into seven, 37, and 13 genotypes, respectively, from 79 strains, based on the combination pattern of constructing units in the polymorphic regions, respectively (Haghighi et al. 2002, 2003). The most kinds of mutation units were observed in locus 1–2, although the most kinds of genotype have been reported in the SREHP gene. In all polymorphic loci, most mutated units that were observed in EHMfas1 and P19-061405 were shared as simian *E. histolytica*-like strain-specific units, including deletions, among EHMfas1 and P19-061405. These mutated units had single-nucleotide substitutions relative to the corresponding units in *E. histolytica*. On the other hand, unshared mutated units were also observed. In the SREHP gene, SN16 was not observed in P19-061405, and the second insertion unit (GATGAA-GAA; DEE) was only observed in EHMfas1. In locus 1–2, 8L2 was specific for EHMfas1. The EHMfas1-specific insertion unit was likely derived from the non-repeating SN3 (GATGAAGAT; DED), with a single-nucleotide substitution. These slight disparities may reflect the differences between the host monkey species or the habitats of EHMfas1 and P19-061405; however, not enough strains have been studied to date. Analyses of these polymorphic loci also indicated that simian *E. histolytica*-like strains can also be classified by genotyping with original mutated units as *E. histolytica*.

It is interesting that *E. dispar* exhibit the same repetitive units as *E. histolytica* in the chitinase (CN2, CN4, and CN6) and the SREHP (SN8 and SN16) genes (Ghosh et al. 2000). Although *E. dispar* exhibits *E. dispar*-specific units, most of those mutated units were not repetitive. On the other hand, EHMfas1 and P19-061405 exhibited many repetitive mutated units, CN3, CN5, CN7, SN9, and SN17. EHMfas1 and P19-061405 exhibited not only mutated CN3 and SN17 but also the corresponding CN2 and SN16. However, all CN4, CN6, and SN8 were changed to CN5, CN7, and SN9. These findings indicate that *E. histolytica* is more closely related to *E. dispar* than the simian *E. histolytica*-like strains, in contrast to the results of other sequence analyses. It is considered that these contradictory findings are probably caused by specific effects, other than general evolution, because SREHP, in particular, is known to be a trophozoite surface antigen (Stanley et al. 1995). In other words, these contradictory findings may indicate differences in the manner of immune escape between different host species. On the other hand, locus 1–2 is a non-coding region and has the most kinds of mutation units. These polymorphic loci must be exposed to other evolutionary effects. This specific contradictory finding is likely a consequence of "concerted evolution" (Dover 1982, 1993; Dover and Tautz 1986; Wilkinson and Chapman 1991; Jinks-Robertson and Petes 1993; Liao 1999).

Concerted evolution is a universal biological phenomenon for repetition of DNA elements and has been observed in many repetitive DNA sequences and multi-gene families. Concerted evolution is thought to result from various mechanisms of DNA turnover, including unequal crossing-over, DNA amplification, gene conversion, and replication slippage. In *Entamoeba* species, concerted evolution has been discussed as it relates to the 5.8S rRNA gene and rRNA-linked *E. histolytica* short tandem repeats (Som et al. 2000; Tawari et al. 2008). It is suggested that diversification of the chitinase gene, the SREHP gene, and locus 1–2 can be caused by replication slippage (Ghosh et al. 2000; Bhattacharya et al. 2005). The repetitive units developing by concerted evolution are homogeneous within species, but differ somewhat between species. The similarities of each kind of unit in the chitinase and SREHP genes, locus 1-2 within simian *E. histolytica*-like strains or *E. histolytica*, and the differences of those between the both are accountable by concerted evolution. Concerted evolution of these polymorphic loci indicates that the repetitive simian *E. histolytica*-like strain-specific units had been amplified and conserved according to speciation as opposed to general DNA evolution, whereas some of these units had been eliminated or were not apparent in *E. histolytica* and *E. dispar*.

Tachibana et al. (2007) proposed that P19-061405 should be distinguished from *E. histolytica* by revival of the named *E. nuttalli* (Castellani 1908). Because EHMfas1 exhibited slight differences but had the same genetic characteristics as P19-061405, EHMfas1 also should be identified as *E. nuttalli*. This study indicates that *E. nuttalli* is endemic to monkey but we cannot exclude the possibility of zoonotic infection from monkey to human. We believe that further comparative study of *E. nuttalli* will contribute to more insights into the phylogeny and pathogenicity of *Entamoeba* species because *E. nuttalli* is very closely related to *E. histolytica* and *E. nuttalli* is the only pathogenic species other than *E. histolytica* among the *Entamoeba* species.

Acknowledgment This work was supported by a Grant-in-Aid for Scientific Research from the Japanese Society for the Promotion of Science.

References

Ali IKM, Zaki M, Clark CG (2005) Use of PCR amplification of tRNA gene-linked short tandem repeats for genotyping *Entamoeba histolytica*. J Clin Microbiol 43:5842–5847

Ayeh-Kumi PF, Ali IM, Lockhart LA, Gilchrist CA, Petri WA Jr, Haque R (2001) *Entamoeba histolytica*: genetic diversity of

clinical isolates from Bangladesh as demonstrated by polymorphisms in the serine-rich gene. Exp Parasitol 99:80–88

Bakatselou C, Beste D, Kadri AO, Somanath S, Clarc CG (2003) Analysis of genes of mitochondrial origin in the genus *Entamoeba*. J Eukaryot Microbiol 50:210–214

Bhattacharya D, Haque R, Singh U (2005) Coding and noncoding genomic regions of *Entamoeba histolytica* have significantly different rates of sequence polymorphisms: implications for epidemiological studies. J Clin Microbiol 43:4815–4819

Castellani A (1908) Note on a liver abscess of amoebic origin in a monkey. Parasitology 1:101–102

Clark CG, Diamond LS (1993) *Entamoeba histolytica*: a method for isolate identification. Exp Parasitol 77:450–455

Clark CG, Diamond LS (1997) Inraspecific variation and phylogenetic relationships in the genus *Entamoeba* as revealed by riboprinting. J Euk Microbiol 44:142–154

Clark CG, Kaffashian F, Tawari B, Windsor JJ, Twigg-Flesner A, Davies-Morel MC, Blessmann J, Ebert F, Peschel B, Le Van A, Jackson CJ, Macfarlane L, Tannich E (2006) New insights into the phylogeny of *Entamoeba* species provided by analysis of four new small-subunit rRNA genes. Int J Syst Evol Microbiol 56:2235–2239

Diamond LS, Harlow DR, Cunnick CC (1978) A new medium for the axenic cultivation of *Entamoeba histolytica* and other *Entamoeba*. Trans R Soc Trop Med Hyg 72:431–432

de la Vega H, Specht CA, Semio CE, Robbins PW, Eichinger D, Caplivski D, Ghosh S, Samuelson J (1997) Cloning and expression of chitinases of *Entamoebae*. Mol Biochem Parasitol 85:139–147

Dover G (1982) Molecular drive: a cohesive mode of species evolution. Nature 299:111–117

Dover GA (1993) Evolution of genetic redundancy for advanced players. Curr Opin Genet Dev 3:902–910

Dover GA, Tautz D (1986) Conservation and divergence in multigene families: alternatives to selection and drift. Philos Trans R Soc Lond B Biol Sci 312:275–289

Ghosh S, Frisardi M, Ramirez-Avila DS, Sturm-Ramirez K, Newton Sanchez OA, Sntos-Preciado JI, Ganguly C, Lohia A, Reed S, Samuelson J (2000) Molecular epidemiology of *Entamoeba* spp.: evidence of a bottleneck (Demographic Sweep) and transcontinental spread of diploid parasites. J Clin Microbiol 38:3815–3821

Haghighi A, Kobayashi S, Takeuchi T, Masuda G, Nozaki T (2002) Remarkable genetic polymorphism among *Entamoeba histolytica* isolates from a limited geographic area. J Clin Microbiol 40:4081–4090

Haghighi A, Kobayashi S, Takeuchi T, Thammapalerd N, Nozaki T (2003) Geographic diversity among genotypes of *Entamoeba histolytica* field isolates. J Clin Microbiol 41:3748–3756

Jinks-Robertson S, Petes TD (1993) Experimental determination of rates of concerted evolution. Methods Enzymol 224:631–646

Kohler S, Tannich E (1993) A family of transcripts (K2) of *Entamoeba histolytica* contains polymorphic repetitive regions with highly conserved elements. Mol Biochem Parasitol 59:49–58

Li E, Kunz-Jenkins C, Stanley SL Jr (1992) Isolation and characterization of genomic clones encoding a serine-rich *Entamoeba histolytica* protein. Mol Biochem Parasitol 50:355–358

Liao D (1999) Concerted evolution: molecular mechanism and biological implications. Am J Hum Genet 64:24–30

Saitou N, Nei M (1987) The neighbor-joining method: a new method for reconstructing phylogenetic trees. Mol Biol Evol 4:406–425

Silberman JD, Clark CG, Diamond LS, Sogin ML (1999) Phylogeny of the genera *Entamoeba* and *Endolimax* as deduced from small-subunit ribosomal RNA sequence. Mol Biol Evol 16:1740–1751

Som I, Azam A, Bhattacharya A, Bhattacharya S (2000) Inter- and intra-strain variation in the 5.8S ribosomal RNA and internal transcribed spacer sequences of *Entamoeba histolytica* and comparison with *Entamoeba dispar*, *Entamoeba moshkovskii* and *Entamoeba invadens*. Int J Parasitol 30:723–728

Stanley SL Jr, Becker A, Kunz-Jenkins C, Foster L, Li E (1990) Cloning and expression of a membrane antigen of *Entamoeba histolytica* possessing multiple tandem repeats. Proc Natl Acad Sci U S A 87:4976–4980

Stanley SL Jr, Tian K, Koester JP, Li E (1995) The serine-rich *Entamoeba histolytica* protein is a phosphorylated membrane protein containing O-linked terminal N-acetylglucosamine residues. J Biol Chem 270:4121–4126

Suzuki J, Kobayashi S, Murata R, Yanagawa Y, Takeuchi T (2007) Profiles of a pathogenic *Entamoeba histolytica*-like variant with variations in the nucleotide sequence of the small subunit ribosomal RNA isolated from a primate (De Brazza's guenon). J Zoo Wildl Med 38:471–474

Tachibana H, Kobayashi S, Kato Y, Nagakura K, Kaneda Y, Takeuchi T (1990) Identification of a pathogenic isolate-specific 30, 000-Mr antigen of Entamoeba histolytica by using a monoclonal antibody. Infect Immun 58:955–960

Tachibana H, Yanagi T, Pandey K, Cheng XJ, Kobayashi S, Sherchand JB, Kanbara H (2007) An *Entamoeba* sp. strain isolated from rhesus monkey is virulent but genetically different from *Entamoeba histolytica*. Mol Biochem Parasitol 153:107–114

Takano J, Narita T, Tachibana H, Shimizu T, Komatsubara H, Terao K, Fujimoto K (2005) *Entamoeba histolytica* and *Entamoeba dispar* infections in cynomolgus monkeys imported into Japan for research. Parasitol Res 97:255–257

Takano J, Narita T, Tachibana H, Terao K, Fujimoto K (2007) Comparison of *Entamoeba histolytica* DNA isolated from a cynomolgus monkey with human isolates. Parasitol Res 101:539–546

Tawari B, Ali IK, Scott C, Quail MA, Berriman M, Hall N, Clark CG (2008) Patterns of evolution in the unique tRNA gene arrays of the genus *Entamoeba*. Mol Biol Evol 25:187–198

Thompson JD, Gibson TJ, Plewniak F, Jeanmougin F, Higgins DG (1997) The ClustalX windows interface: flexible strategies for multiple sequence alignment aided by quality analysis tools. Nucleic Acids Research 25:4876–4882

Verweij JJ, Vermeer J, Brienen EAT, Blotkamp C, Laeijendecker D, Lieshout LV, Polderman AM (2003) *Entamoeba histolytica* infections in captive primates. Parasitol Res 90:100–103

Wilkinson GS, Chapman AM (1991) Length and sequence variation in evening bat D-loop mtDNA. Genetics 128:607–617

Zaki M, Clark CG (2001) Isolation and characterization of polymorphic DNA from *Entamoeba histolytica*. J Clin Microbiol 39:897–905

Zaki M, Meelu P, Sun W, Clark CG (2002) Simultaneous differentiation and typing of *Entamoeba histolytica* and *Entamoeba dispar*. J Clin Microbiol 40:1271–1276

Functional B7.2 and B7-H2 Molecules on Myeloma Cells Are Associated with a Growth Advantage

Taishi Yamashita,[1,3] Hideto Tamura,[1] Chikako Satoh,[1,4] Eiji Shinya,[2] Hidemi Takahashi,[2] Lieping Chen,[5] Asaka Kondo,[1] Takashi Tsuji,[3] Kazuo Dan,[1] and Kiyoyuki Ogata[1]

Abstract

Purpose: B7 family molecules expressed on antigen-presenting cells stimulate or inhibit normal immune responses. The aim of this study was to investigate whether functional B7.2 and B7-H2 molecules are expressed on myeloma cells and, if so, whether they are associated with pathophysiology in myeloma.

Experimental Design: The expression of B7.2 and B7-H2 molecules on normal plasma and neoplastic (myeloma) plasma cells was analyzed. The cell proliferation and immunomodulatory function of myeloma cells related to B7.2 and B7-H2 expression were examined.

Results: Human myeloma cell lines commonly expressed B7.2 and B7-H2 molecules. B7.2 expression on plasma cells was more common in myeloma patients ($n = 35$) compared with that in patients with monoclonal gammopathy of unknown significance ($n = 12$) or hematologically normal individuals ($n = 10$). Plasma cells expressing B7-H2 were observed in myeloma patients alone, although rarely. Patients whose myeloma cells showed high B7.2 expression were more anemic and thrombocytopenic than other myeloma patients. The expression of these molecules was induced or augmented by cultivating myeloma cells with autologous stroma cells or tumor necrosis factor-α, a key cytokine in myeloma biology. Cell proliferation was more rapid in the $B7.2^+$ and $B7\text{-}H2^+$ populations compared with the $B7.2^-$ and $B7\text{-}H2^-$ populations, respectively, in the human myeloma cell lines examined. B7.2 and B7-H2 molecules on myeloma cells induced normal $CD4^+$ T cells to proliferate and produce soluble factors, including interleukin-10 that stimulate myeloma cell proliferation.

Conclusions: Functional B7.2 and B7-H2 molecules detected on myeloma cells may be involved in the pathophysiology of myeloma.

Multiple myeloma (MM) is a virtually incurable hematologic malignancy characterized by monoclonal growth of plasma cells (myeloma cells). In addition to the well-known deficiency in B-cell immunity, T-cell dysfunction, such as reduced cytotoxic activity (1) and reduced responsiveness to interleukin 2 (IL-2; refs. 2, 3), has been reported, which may weaken antitumor immune responses in MM patients. The interaction between myeloma cells and bone marrow (BM) stroma cells stimulates the production of a variety of cytokines that are involved in the pathophysiology of MM (4, 5). Those include IL-6, IL-10, and tumor necrosis factor-α (TNF-α), which stimulate myeloma cell growth (6–9). An interesting aspect is that both IL-10 and TNF-α have an immunomodulating function, including inhibition of CTLs (10–12).

The B7 family molecules play an important role in the immune response by costimulating or coinhibiting T cells via antigen-T-cell receptor interactions (13–16). Interactions between B7.1/B7.2 ligands on professional antigen-presenting cells and CD28/CTLA-4 receptors on T cells represent a classic pathway and control antigen-specific T-cell proliferation, anergy, and survival. B7-H2 is another B7 family molecule induced by TNF-α (17). The binding of B7-H2 to the inducible costimulatory receptor (ICOS), a counterreceptor, induces T cells to proliferate and secrete both Th1 and Th2 cytokines, such as IFN-γ and IL-4 but not the potent Th1 cytokine IL-2 (18). Furthermore, the B7-H2-ICOS signal induces IL-10 production, which plays an important role in reducing immune responses (19, 20). B7 family molecules are expressed not only on professional antigen-presenting cells but also on some tumor cells and the latter may modulate antitumor immunity in hosts. For example, we detected the expression of B7.2 and B7-H2 molecules on blasts from patients with acute myeloid leukemia and showed that these molecules on acute myeloid

Authors' Affiliations: [1]Division of Hematology, Department of Medicine and [2]Department of Microbiology and Immunology, Nippon Medical School, Tokyo, Japan; [3]Department of Biological Science and Technology, Tokyo University of Science, Chiba, Japan; [4]Department of Bioregulation, Institute of Development and Aging Science, Nippon Medical School, Kawasaki, Japan; and [5]Department of Dermatology, Department of Oncology and Institute for Cell Engineering, Johns Hopkins University School of Medicine, Baltimore, Maryland

Received 2/24/08; revised 10/21/08; accepted 10/25/08.

Grant support: A Grant-in-Aid for Scientific Research from the Japan Society for the Promotion of Science (no. 20591157).

The costs of publication of this article were defrayed in part by the payment of page charges. This article must therefore be hereby marked *advertisement* in accordance with 18 U.S.C. Section 1734 solely to indicate this fact.

Note: Supplementary data for this article are available at Clinical Cancer Research Online (http://clincancerres.aacrjournals.org/).

Requests for reprints: Hideto Tamura, Division of Hematology, Department of Medicine, Nippon Medical School, 1-1-5 Sendagi, Bunkyo-ku, Tokyo 113-8603, Japan. Phone: 81-3-3822-2131; Fax: 81-3-5685-1793; E-mail: tam@nms.ac.jp.

doi:10.1158/1078-0432.CCR-08-0501

Translational Relevance

Multiple myeloma (MM) is a virtually incurable hematologic malignancy. Therefore, research that could result in improved MM treatment and/or a breakthrough in our understanding of this disease is very important. This article shows that myeloma cells from a substantial number of MM patients express functional B7.2 or B7-H2 molecules. Furthermore, it provides evidence that these molecules on myeloma cells may be involved in the pathophysiology of the disease. It is anticipated that these data will be translated into a new therapeutic strategy for MM.

leukemia blasts inhibited anti-acute myeloid leukemia immunity *in vitro* and were associated with poor patient prognosis (21). In MM, data on B7 family molecules are lacking. To the best of our knowledge, only one study examined this topic. Pope et al. (22) observed that MM patients whose tumor cells expressed B7.2 molecules had a poor prognosis. However, they did not examine whether the B7.2 molecules on myeloma cells were functional. Here, we investigated whether functional B7.2 and B7-H2 molecules are expressed on myeloma cells and, if so, whether these B7 molecules are associated with pathophysiology in MM.

Materials and Methods

Cell lines. Eleven human myeloma cell lines (HMCL), KMM-1, KMS-11, KMS-12BM, KMS-12PE, KMS-18, KMS-20, KMS-26, KMS-27, KMS-28BM, KMS-28PE, and KMS-34, were kindly provided by Dr. Otsuki (Kawasaki Medical School, Okayama, Japan). PCM6 cells were obtained from the Riken Cell Bank, and RPMI8226 and U266 cells were from the American Type Culture Collection. PCM6 cells were maintained in McCoy's 5A modified medium (Life Technologies) containing 20% FCS and 3 ng/mL of recombinant IL-6 (Kirin Brewery Co.). The other cells were maintained in complete medium, i.e., RPMI 1640 supplemented with 10% FCS and 2 mmol/L L-glutamine. In experiments examining the effects of cytokines on these cells, TNF-α

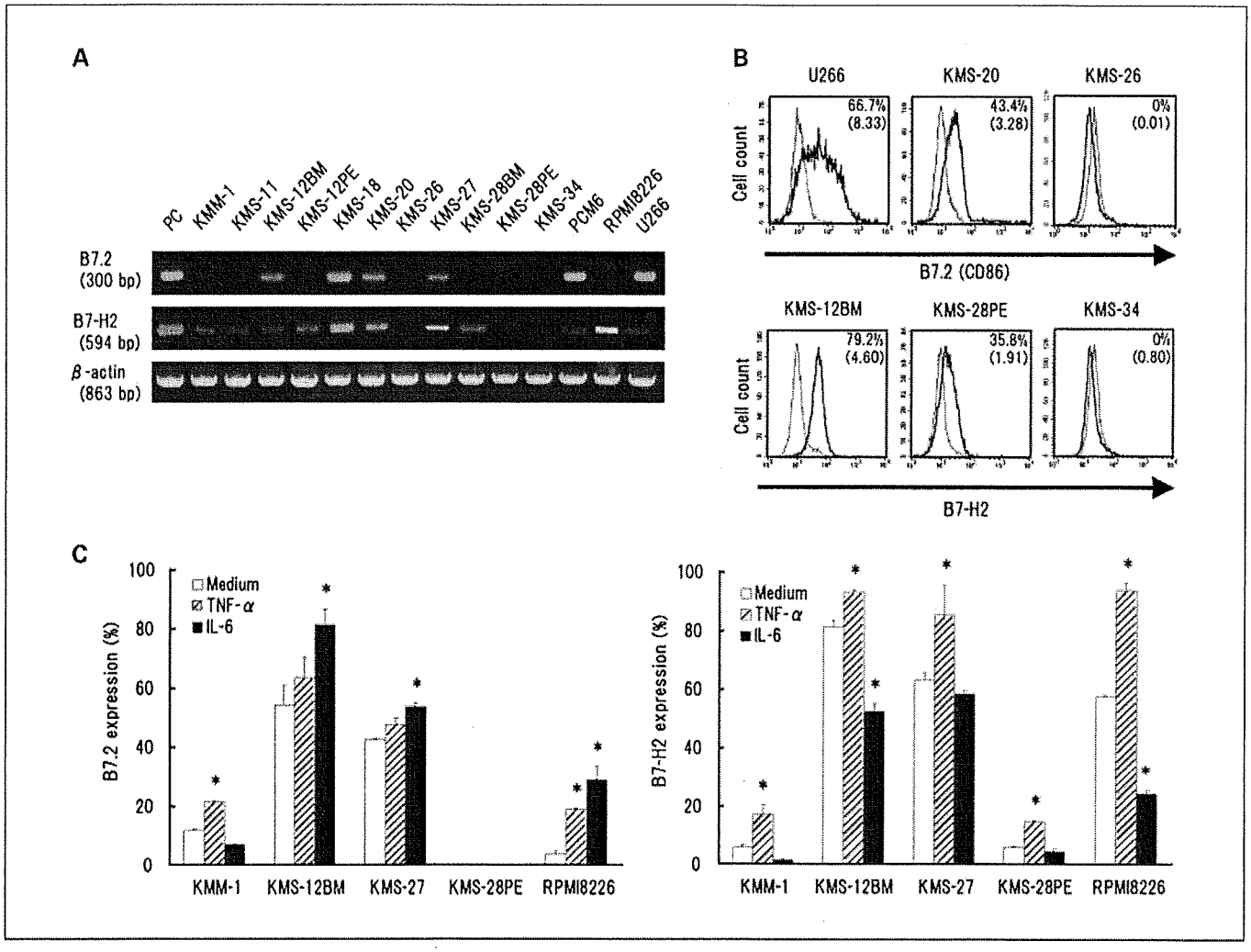

Fig. 1. *A,* B7.2 and B7-H2 mRNA expression analyzed using reverse transcription-PCR in 14 HMCLs. Equal amounts of cDNA from each cell line were amplified using primers specific for B7.2, B7-H2, and β-actin. *B,* representative flow cytometry analyses of the B7.2 and B7-H2 expression in HMCLs. Bold curves, staining with anti-B7.2 or anti-B7-H2 mAb; thin curves, staining with isotype-matched control immunoglobulin. Data are expressed in the percentages of positive cells and in relative mean fluorescence intensity (*numbers in parentheses*). *C,* effects of TNF-α and IL-6 on B7.2 and B7-H2 expression in HMCLs. Columns, mean of three independent experiments; bars, SD. Medium, no cytokine was added. *, $P < 0.05$, significantly different from Medium.

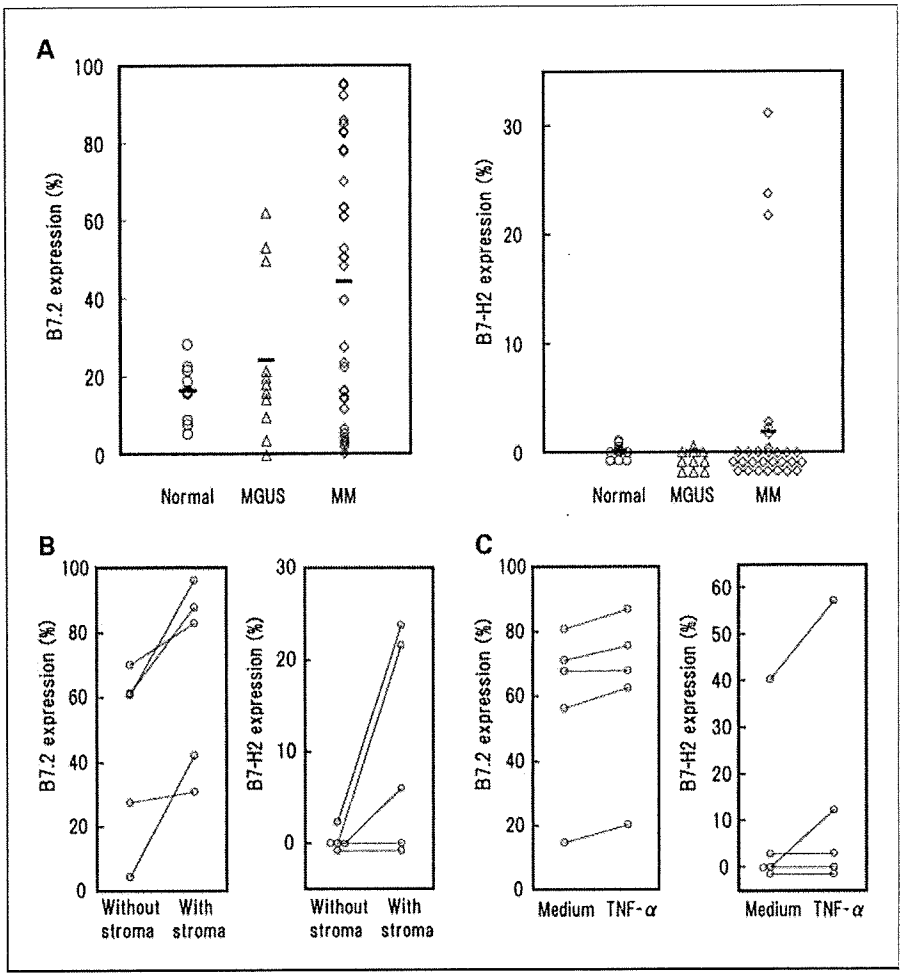

Fig. 2. *A*, percentages of B7.2$^+$ and B7-H2$^+$ plasma cells among all plasma cells in 10 hematologically normal individuals and 12 monoclonal gammopathy of unknown significance and 35 MM patients determined using flow cytometry. Horizontal bars, mean. Effects of autologous stroma cells (*B*) and TNF-α (*C*) on B7.2 and B7-H2 expression on myeloma cells from patients.

(500 units/mL; PeproTech), IL-10 (10 ng/mL; MBL), or IL-6 (10 ng/mL) were added to the cultures. The cell number was counted using the trypan blue dye-exclusion method.

In some experiments, B7.2$^+$, B7.2$^-$, B7-H2$^+$, or B7-H2$^-$ KMS-27 cells were purified with FACSVantage (Becton Dickinson) as described previously (23).

Patients, hematologically normal individuals, and cell preparation. BM samples were obtained from individuals who underwent BM aspiration for diagnostic purposes after obtaining written informed consent. They included 35 MM patients [4 stage I and 31 stage III according to the definition of Durie and Salmon (24)], 12 patients with monoclonal gammopathy of unknown significance, and 10 hematologically normal individuals. All BM samples from MM patients were obtained at the initial diagnosis, except for those from 6 patients, 2 of whose samples showed that they were refractory to conventional chemotherapy and 4 of whose samples were in the plateau phase according to the standard definition. Diagnoses were made according to the WHO classification. Mononuclear cells were separated from BM samples with Histopaque (Sigma) density centrifugation. These cells were used immediately or cryopreserved in liquid nitrogen until use. In cell samples from hematologically normal individuals, CD19-positive cells were enriched from BM mononuclear cells using magnetic cell sorting (Miltenyi Biotec; ref. 23) to ensure plasma cell identification in flow cytometry (25). This study was approved by the institutional review board of Nippon Medical School.

Stroma cells were prepared as follows. BM mononuclear cells from MM patients (2×10^6/mL) were plated in 6-well plates in complete medium. The cultures were fed weekly by removing 75% of the medium and adding fresh medium to make up the same volume. After the cultivated cells became adherent, stromal cell shaped, positive for mesenchymal stem cell markers (CD44 and CD90), and negative for hematopoietic markers (CD34, CD45, and CD11b), they were used as stroma cells (26). In experiments inducing B7.2 and B7-H2 expression, mononuclear cells were cultured in complete medium on autologous stroma cells for 3 wk or with TNF-α (500 units/mL) for 2 d.

Reverse transcription-PCR. Total RNA extracted from each HMCL was reverse transcribed with Superscript II Reverse transcriptase (Invitrogen) using random hexamers. PCR amplification was done using the primer sets for B7.2 and B7-H2 and PCR conditions previously described (21).

Flow cytometry. Immunophenotyping was done with FACScan (Becton Dickinson; refs. 21, 27). Briefly, after blocking with human immunoglobulin, patient BM samples were stained with anti-CD38 monoclonal antibody (mAb) labeled with FITC and phycoerythrin-labeled anti-B7.2 (Becton Dickinson) or anti-B7-H2 mAb (e-Bioscience). Plasma cells were identified by a high expression of CD38 molecules (22). We also confirmed that the identified plasma cells expressed another plasma cell marker, CD138 (Becton Dickinson). Examples of flow cytometry analysis are shown in Supplementary Fig. S1. HMCLs were single stained with FITC/phycoerythrin–conjugated mAbs against lymphocyte function–associated antigen-1 (LFA-1), intercellular adhesion molecule-1 (ICAM-1; Beckman Coulter), very late antigen-4, vascular cell adhesion molecule-1 (Becton Dickinson), B7.2, and B7-H2.

Cell cycle analysis. After blocking with human immunoglobulin, HMCLs were stained with purified mouse anti-B7.2 or anti-B7-H2

mAbs. The cells were washed and further incubated with FITC-conjugated antimouse IgG (Biosource). Then, the cells were fixed with 70% ethanol at 4°C for 3 h. The fixed cells were washed and resuspended in 100 μL of PBS and 1 μg of RNase (Qiagen) containing 0.1 mg/mL of propidium iodide (Sigma). The cell cycle profiles of B7.2$^+$, B7.2$^-$, B7-H2$^+$, and B7-H2$^-$ HMCLs were analyzed using flow cytometry.

Colony-forming assay. Purified B7.2$^+$, B7.2$^-$, B7-H2$^+$, and B7-H2$^-$ cells (1×10^3 per culture dish) were cultured in MethoCult H4230 methylcellulose medium (StemCell Technologies; ref. 23). Colonies (aggregates of 50 or more cells) were scored on day 14 of culture.

Mixed lymphocyte-myeloma reaction. CD4$^+$ T cells (purity > 95%) were prepared from peripheral blood of healthy volunteers on magnetic cell sorting columns (21). These cells (1×10^5) were cocultured with irradiated (20,000 rad) myeloma cells (1×10^5) expressing both B7.2 and B7-H2 molecules in microtiter wells for 5 d. Antagonistic mAbs (10 μg/mL) against B7.2 and ICOS (e-Bioscience) were added to the cultures to block the B7.2-CD28 and B7-H2-ICOS pathways, respectively. During the final 18 h of culture, [^{3}H]thymidine (1 μCi/well) was added to determine T-cell proliferation. All samples were assayed at least in quadruplicate.

In some experiments, culture supernatants of mixed lymphocyte-myeloma reaction (MLMR) were collected on day 5 of culture. The

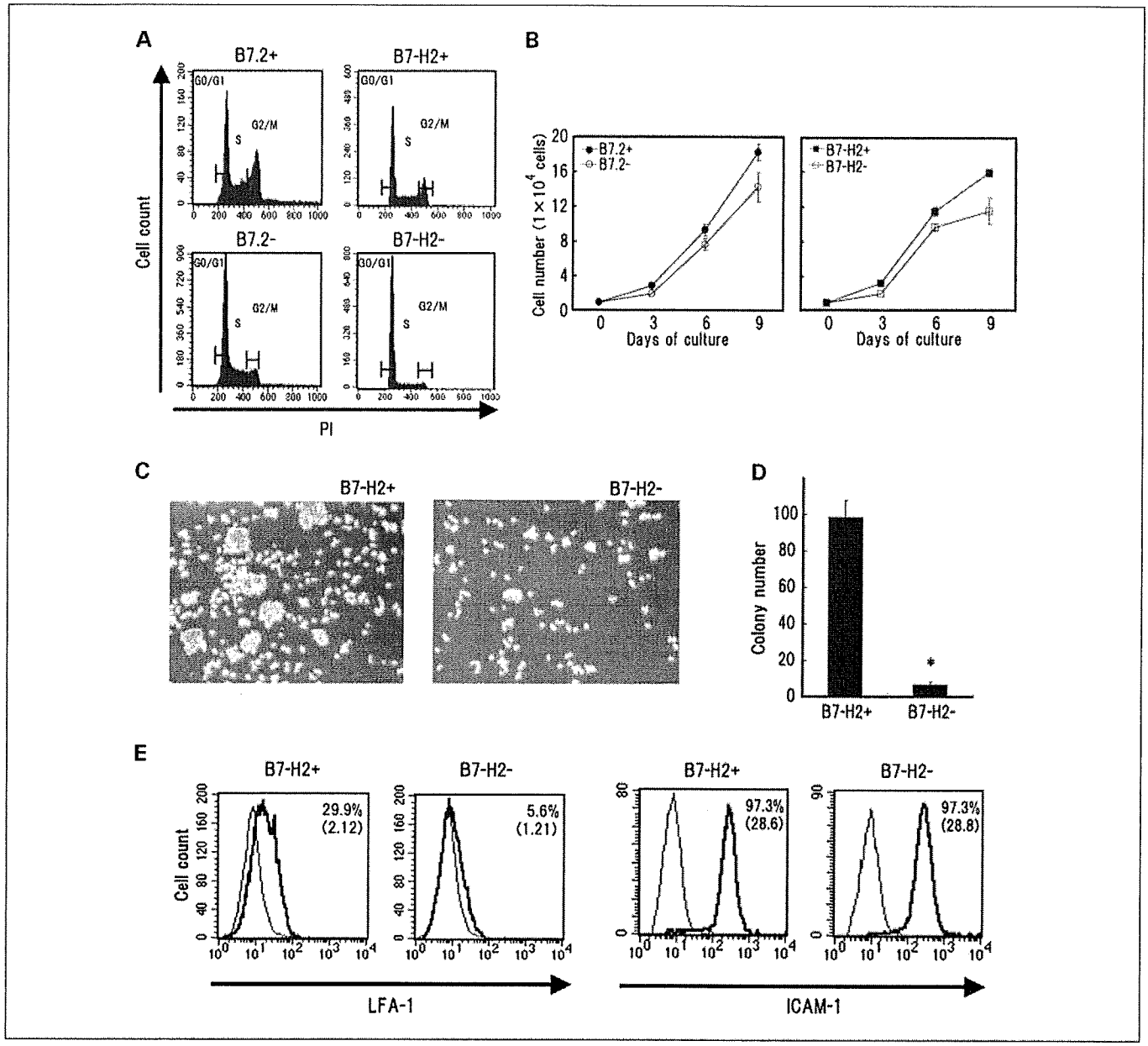

Fig. 3. *A,* cell cycle analyses of B7.2$^+$ or B7.2$^-$ KMS-27 cells (*left*) and of B7-H2$^+$ or B7-H2$^-$ KMS-27 cells (*right*). Each cell population was gated and analyzed in flow cytometry. Analysis on at least 10,000 events for each sample. The cell cycle data were reproducible when B7-H2$^+$ and B7-H2$^-$ KMS-27 cells isolated using FACSVantage were analyzed (data not shown). *B,* proliferation of isolated B7.2$^+$ or B7.2$^-$ KMS-27 cells and B7-H2$^+$ or B7-H2$^-$ KMS-27 cells. Points, mean of three independent experiments; bars, SD. *C,* photomicrographs of purified B7-H2$^+$ and B7-H2$^-$ KMS-27 cells during exponential cell growth in culture. *D,* number of colonies (defined as aggregates composed of 20 or more cells) formed by purified B7-H2$^+$ and B7-H2$^-$ cells on day 7 of culture. Columns, mean of three independent triplicate cultures; bars, SD. *, $P < 0.01$ compared with the data of B7-H2$^+$. *E,* representative flow cytometry analyses of LFA-1 and ICAM-1 expression on B7-H2$^+$ and B7-H2$^-$ KMS-27 cells. Bold curves, staining with anti – LFA-1 or anti – ICAM-1 mAb; thin curves, staining with isotype-matched control immunoglobulin. Data are expressed in percentages of positive cells and in relative mean fluorescence intensity (*numbers in parentheses*).